

Department of Mathematics and Statistics

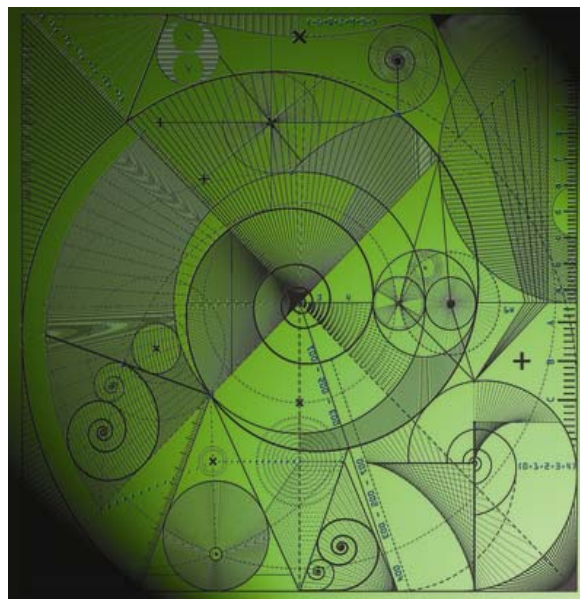
Preprint MPS-2012-04

28 May 2012

A High Frequency Boundary Element Method for Scattering by a Class of Nonconvex Obstacles

by

S. N. Chandler-Wilde, D. P. Hewett, S. Langdon
and A. Twigger



A high frequency boundary element method for scattering by a class of nonconvex obstacles

S. N. Chandler-Wilde · D. P. Hewett · S. Langdon · A. Twigger

Received: date / Accepted: date

Abstract In this paper we propose and analyse a hybrid numerical-asymptotic boundary element method for the solution of problems of high frequency acoustic scattering by a class of sound-soft nonconvex polygons. The approximation space is enriched with carefully chosen oscillatory basis functions; these are selected via a study of the high frequency asymptotic behaviour of the solution. We demonstrate via a rigorous error analysis, supported by numerical examples, that to achieve any desired accuracy it is sufficient for the number of degrees of freedom to grow only in proportion to the logarithm of the frequency as the frequency increases, in contrast to the at least linear growth required by conventional methods. This appears to be the first such numerical analysis result for any problem of scattering by a nonconvex obstacle.

Keywords High frequency scattering · Boundary Element Method · Helmholtz equation

1 Introduction

There has been considerable interest in recent years in the development of numerical methods for time harmonic acoustic and electromagnetic scattering problems that are able to efficiently resolve the scattered field at high frequencies. Standard finite or boundary element methods, with piecewise polynomial approximation spaces, suffer from the restriction that a fixed number of degrees of freedom is required per wavelength in order to represent the oscillatory solution, leading to excessive computational cost when the scatterer is large compared to the wavelength.

Department of Mathematics and Statistics, University of Reading, Whiteknights PO Box 220, Reading RG6 6AX, UK.
Tel: +44-118-3785012
Fax: +44-118-9313423
E-mail: d.p.hewett@reading.ac.uk.
Supported by EPSRC grant EP/F067798/1.

A methodology that has shown a great deal of promise is the so-called “hybrid numerical-asymptotic” approach, where partial knowledge of the high frequency asymptotic behaviour is incorporated into the approximation space. This approach is particularly attractive when employed within a boundary element method (BEM) framework, since knowledge of the high frequency asymptotics is required only on the boundary of the scatterer. Whereas conventional BEMs for two-dimensional (2D) problems require the number of degrees of freedom to grow at least linearly with respect to frequency in order to maintain a prescribed level of accuracy as the frequency increases, hybrid numerical-asymptotic BEMs have been shown, for a range of problems, to require a significantly milder (often only logarithmic) growth in computational cost. We refer to [14] (and the very many references therein) for a review of this fast-evolving field and its historical development.

The key idea behind this approach is to reformulate the boundary value problem (defined precisely in §2) as a boundary integral equation, with frequency dependent solution V , and then to approximate V using an ansatz of the form

$$V(x, k) \approx V_0(x, k) + \sum_{m=1}^M V_m(x, k) \exp(ik\psi_m(x)), \quad x \in \Gamma, \quad (1)$$

where k (the wavenumber) is proportional to the frequency of the incident wave, and Γ is the boundary of the scatterer. In this representation, V_0 is a known (generally oscillatory) function (derived from the high frequency asymptotics), the phases ψ_m are chosen *a-priori* and the amplitudes V_m , $m = 1, \dots, M$, are approximated numerically. If V_0 and ψ_m , $m = 1, \dots, M$, are chosen wisely, then $V_m(\cdot, k)$, $m = 1, \dots, M$, will be much less oscillatory than $V(\cdot, k)$ and so can be better approximated by piecewise polynomials than V itself.

For scattering by convex obstacles, approaches in this vein were suggested already in the 1970s [39] (and see [14] and the references therein). The first numerical analysis, for a scheme for scattering by a smooth convex obstacle, appeared in the mid 1990s [2] ([26] is a recent, very effective and fully discrete 3D solver in the same spirit). In the last 5-10 years algorithms have been developed for classes of 2D problems that achieve user-specified accuracies with a number of degrees of freedom that remains fixed or grows at worst logarithmically as the frequency increases. Specifically, [18, 32, 22] tackle problems of scattering by perfectly reflecting or impedance strips, [10, 23] smooth convex obstacles, and [16, 33, 17, 28] convex polygons and convex curvilinear polygons. In parallel with these algorithmic developments new tools have been developed which lead to a complete numerical analysis of many of these algorithms [18, 32, 23, 16, 17, 36, 28]. However, to date, the vast majority of algorithms, and all the numerical analysis, have been restricted to problems of scattering by single convex obstacles.

The main difficulty in moving from the convex case to the nonconvex case is that the high frequency asymptotic behaviour of the solution, knowledge of which is required for the design of the hybrid approximation space (via the choice of V_0 and ψ_m in (1)), is significantly more complicated for nonconvex scatterers than for convex scatterers. In the context of polygonal scatterers in 2D two additional complexities are illustrated in Figure 1, where the real part of the total field is plotted for the case where a plane wave is incident on a sound-soft nonconvex polygon (full details of these configurations are provided in §7).

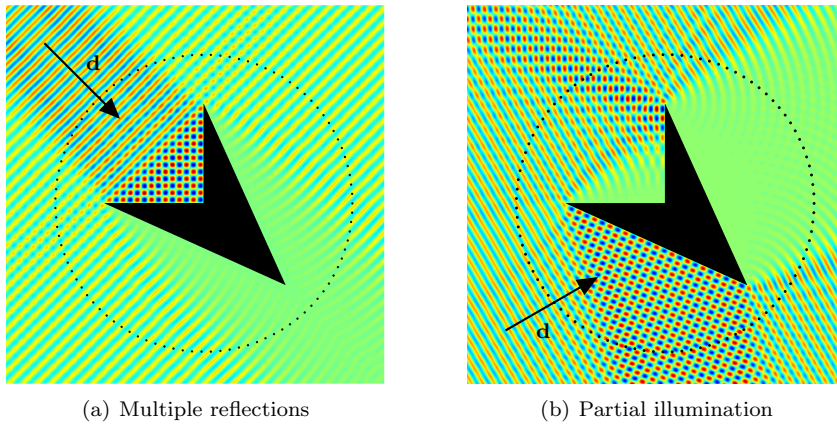


Fig. 1 Plots of the real part of the total field for scattering of a plane wave by a sound-soft nonconvex polygon for two directions of incidence \mathbf{d} (exact dimensions are given in §7; the circle surrounding the scatterer is used for the computation of errors in the total field, see Figure 8).

First, there is the possibility that multiply-reflected and diffracted-reflected rays are present in the asymptotic solution, as shown in Figure 1(a). (These do not occur in the convex case, where all reflected rays propagate to infinity without further interaction with the scatterer.) Second, there is the possibility of partial illumination of a side of the polygon, as shown in Figure 1(b). To explain this more fully, we note that in the schemes proposed for the convex polygon case in [16, 17, 28], the sides of the polygon are classified according to whether they are “illuminated” or “in shadow” with respect to the incident wave, with a different approximation space being used on the two types of side. In the case of a nonconvex polygon a side can be partially illuminated and partially in shadow, because of the shadowing effect of another part of the scatterer, as is the case for the vertical side in Figure 1(b). Across this shadow boundary between the illuminated and shadow regions the solution varies smoothly, but increasingly rapidly, as the frequency increases, approaching the jump discontinuity predicted by the geometrical optics approximation in the limit of infinite frequency.

Our approach in dealing with these issues is to consider simple “canonical problems” which encapsulate the behaviour in question. Consideration of the behaviour of the solution to these canonical problems allows us to choose V_0 and ψ_m appropriately in (1) so that V_m , $m = 1, \dots, M$, are slowly oscillating. In the convex polygon case, the canonical problem associated with the reflection of the incident wave by the illuminated sides is that of reflection by an infinite half-plane (cf. [16, pp. 621-622]). In this paper, on a particular class of nonconvex polygons, the canonical problem associated with the issue of multiple reflections is that of scattering in a quarter-plane. The canonical problem associated with the issue of partial illumination is that of diffraction by a knife edge. We elaborate on the relationship between these problems and the class of nonconvex polygons considered in this paper in §3.

Of course, the same issues must be overcome in fully asymptotic methods. Although the original version of the Geometrical Theory of Diffraction (GTD) [29] was deficient in the sense that it did not include the shadow boundary behaviour, more sophisticated, uniform versions of GTD have been developed which capture this [30, 7]. However, we emphasize that, in the numerical-asymptotic approach developed here, we do not require the computation of a full asymptotic solution in order to design our hybrid approximation space. Rather, we need merely a representation of the form (1), with an explicit (and relatively simple) term V_0 and explicit phases ψ_m , that captures the high frequency oscillations present in the solution. To design hybrid algorithms optimally, and prove their effectiveness by rigorous numerical analysis, we need additionally to understand the regularity of the amplitudes V_m , $m = 1, \dots, M$, moreover obtaining bounds on these amplitudes that are explicit in their dependence on the wavenumber. This requires high frequency asymptotics of a new kind which aims at coarser information than the full asymptotic solution. The results of this kind that we require in this paper are proved in §3 and §4 below.

As alluded to above, most high frequency algorithms developed to date have been for convex scatterers. The case of multiple smooth convex scatterers, which shares many of the difficulties associated with single nonconvex scatterers, has been considered in [27, 24, 25, 3]. The key theme of that body of work is a decomposition of the multiple scattering problem into a series of problems of scattering by single convex obstacles, with in each case the incident field consisting of a combination of the original incident field with previously scattered waves. This approach does not generalise easily to single nonconvex scatterers, since the number of terms required in the series increases rapidly as the distance between the separated convex scatterers decreases. It may however provide some insight into how to extend the ideas discussed in this paper to more general nonconvex scatterers, providing as it does algorithms for determining a high frequency ansatz similar to (1) for the oscillatory nature of the solution. An algorithm for multiple scattering by arrays of circular cylinders is proposed in [4], but an extension to non-circular scatterers is not clear as the algorithm relies on the fact that for a single circular scatterer the solution is known explicitly.

An algorithm for single nonconvex scatterers is outlined in [9, 11], and the numerical results presented suggest that it is accurate at high frequencies. This approach is not supported by a rigorous analysis however, and it is not clear how the number of degrees of freedom required to achieve a prescribed accuracy depends on either the frequency or the geometrical configuration of the scatterer. We also mention here the preliminary work in [15], where a brief outline of some of the key steps of the algorithm described in this paper is presented without analysis.

In this paper we show, via rigorous numerical analysis supported by numerical results, that hybrid numerical-asymptotic methods can be as effective for a class of nonconvex polygons as they are for convex polygons. In particular, we build on the work in [28], where a hybrid numerical-asymptotic method was developed for problems of scattering by convex polygons, using an ansatz of the form (1), with V_m , $m = 1, \dots, M$, approximated using an hp approximation space. There it was demonstrated, via a rigorous error analysis supported by numerical results, that to achieve any prescribed level of accuracy it is sufficient for the number of degrees of freedom to grow only logarithmically with respect to frequency, as the

frequency increases. Moreover, it was shown that, when the frequency is fixed, the convergence rate is exponential as a function of the number of degrees of freedom. Here, we use a modified ansatz (again of the form (1)), taking account of the more complicated asymptotic behaviour of the solution. This leads not only to a different form of V_0 , but also requires new phase functions ψ_m , compared to the convex case. However, as for the convex case, we demonstrate that approximating the V_m using an hp approximation space leads to exponential convergence at fixed frequency, and that the number of degrees of freedom needs to grow only logarithmically to maintain accuracy as the frequency increases.

An outline of the paper is as follows. We begin in §2 by stating precisely the problem that we consider in this paper. In §3 we clarify the class of nonconvex polygons for which our analysis holds, and state the exact form of the ansatz (1) that we use. Further, we provide regularity estimates for those parts of the solution (V_m , $m = 1, \dots, M$) that we will approximate numerically. The key to achieving our goal of being able to approximate the solution in an (almost) frequency independent way lies in proving that V_m , $m = 1, \dots, M$, are not oscillatory. That this is true, for an appropriate choice of V_0 and ψ_m , $m = 1, \dots, M$, is one of the main results of this paper (leading as it does to the design of our approximation space), and the proof occupies §4. We define our approximation space in §5, and prove best approximation estimates based on the results obtained in §3. In §6 we describe the Galerkin method that we use, and we combine the results of the earlier sections to derive rigorous k -explicit error estimates for our approximations to the total field and the far field pattern. In §7 we present numerical examples, demonstrating the efficiency and accuracy of our scheme.

2 Problem statement

We focus throughout the paper on the 2D problem of scattering of the time harmonic incident plane wave

$$u^i(\mathbf{x}) := e^{ik\mathbf{x}\cdot\mathbf{d}}, \quad (2)$$

by a sound soft polygon. In (2) $k > 0$ is the wavenumber, $\mathbf{x} = (x_1, x_2) \in \mathbb{R}^2$, and \mathbf{d} is a unit direction vector. Let Ω denote the interior of the polygon, and let $D := \mathbb{R}^2 \setminus \overline{\Omega}$ denote the unbounded exterior domain. The boundary value problem (BVP) we wish to solve is: given the incident field u^i , determine the total field $u \in C^2(D) \cap C(\overline{D})$ such that

$$\Delta u + k^2 u = 0, \quad \text{in } D, \quad (3)$$

$$u = 0, \quad \text{on } \Gamma := \partial\Omega, \quad (4)$$

and $u^s := u - u^i$ satisfies the Sommerfeld radiation condition (see, e.g., [14, (2.9)]). The unique solvability of this BVP is well known (see, e.g., [14, Theorem 2.12]). Standard arguments connecting formulations in classical function spaces to those in a Sobolev space setting (see, e.g., [20, Theorem 3.7] and [14, p. 107]) imply that if u satisfies the above BVP then also $u \in H_{\text{loc}}^1(D)$. From standard elliptic regularity results, it follows moreover that u is C^∞ up to the boundary of ∂D , excluding the corners of the polygon [14, Lemma 2.35].

The starting point of the boundary integral equation (BIE) formulation is that, if u satisfies the BVP then a form of Green's representation theorem holds, namely (see [16] and [14, (2.107)])

$$u(\mathbf{x}) = u^i(\mathbf{x}) - \int_{\Gamma} \Phi_k(\mathbf{x}, \mathbf{y}) \frac{\partial u}{\partial \mathbf{n}}(\mathbf{y}) \, ds(\mathbf{y}), \quad \mathbf{x} \in D, \quad (5)$$

where $\Phi_k(\mathbf{x}, \mathbf{y}) := (i/4)H_0^{(1)}(k|\mathbf{x} - \mathbf{y}|)$ is the fundamental solution for (3), $H_\nu^{(1)}$ the Hankel function of the first kind of order ν , and $\partial u / \partial \mathbf{n}$ is the normal derivative, with \mathbf{n} the unit normal directed into D . We note that, as discussed in [16] and [14, Theorem 2.12], it holds that $\partial u / \partial \mathbf{n} \in L^2(\Gamma)$. It is well known (see, e.g., [14, §2]) that, starting from the representation formula (5), we can derive various BIEs for $\partial u / \partial \mathbf{n} \in L^2(\Gamma)$, each taking the form

$$\mathcal{A} \frac{\partial u}{\partial \mathbf{n}} = f, \quad (6)$$

where $f \in L^2(\Gamma)$ and $\mathcal{A} : L^2(\Gamma) \rightarrow L^2(\Gamma)$ is a bounded linear operator.

In the standard combined potential formulation (see [14, (2.114) and (2.69)]),

$$\mathcal{A} = \mathcal{A}_{k,\eta} := \frac{1}{2}\mathcal{I} + \mathcal{D}'_k - i\eta\mathcal{S}_k, \quad (7)$$

and $f = \partial u^i / \partial \mathbf{n} - i\eta u^i$, where $\eta \in \mathbb{R}$ is a coupling parameter, \mathcal{I} is the identity operator, and the single-layer potential operator \mathcal{S}_k and the adjoint double-layer potential operator \mathcal{D}'_k are defined by

$$\begin{aligned} \mathcal{S}_k \psi(\mathbf{x}) &:= \int_{\Gamma} \Phi_k(\mathbf{x}, \mathbf{y}) \psi(\mathbf{y}) \, ds(\mathbf{y}), \quad \mathbf{x} \in \Gamma, \quad \psi \in L^2(\Gamma), \\ \mathcal{D}'_k \psi(\mathbf{x}) &:= \int_{\Gamma} \frac{\partial \Phi_k(\mathbf{x}, \mathbf{y})}{\partial \mathbf{n}(\mathbf{x})} \psi(\mathbf{y}) \, ds(\mathbf{y}), \quad \mathbf{x} \in \Gamma, \quad \psi \in L^2(\Gamma). \end{aligned}$$

From the results in [21] for C^2 domains, and [16] and [14, Theorem 2.27] for general Lipschitz domains, we know that $\mathcal{A}_{k,\eta}$ is invertible for $k > 0$, and hence the BIE (6) is uniquely solvable, provided $\eta \in \mathbb{R} \setminus \{0\}$. Recent results ([13, (6.10)], [5, Theorem 2.11]), building on earlier work [31], suggest that $\eta = k$ is a good choice for larger k , in that it approximately minimises the condition number of $\mathcal{A}_{k,\eta}$ and its boundary element discretization.

In an important recent theoretical development [36] a new formulation has been derived for the case when Ω is star-like with respect to the origin. This takes the form (6) with

$$\mathcal{A} = \mathcal{A}_k := (\mathbf{x} \cdot \mathbf{n}) \left(\frac{1}{2}\mathcal{I} + \mathcal{D}'_k \right) + \mathbf{x} \cdot \nabla_{\Gamma} \mathcal{S}_k + \left(\frac{1}{2} - ik|\mathbf{x}| \right) \mathcal{S}_k, \quad (8)$$

the so-called ‘‘star-combined’’ potential operator, and $f(\mathbf{x}) = \mathbf{x} \cdot \nabla u^i(\mathbf{x}) + (1/2 - ik|\mathbf{x}|)u^i(\mathbf{x})$. Here ∇_{Γ} is the surface gradient operator. From [36] we know that (for Ω Lipschitz and star-like) \mathcal{A}_k is invertible for all $k > 0$. The point of this new formulation, as shown in [36] and discussed below, is that \mathcal{A}_k is coercive as an operator on $L^2(\Gamma)$, moreover with a coercivity constant which is explicitly known and is wavenumber independent. This implies the invertibility of \mathcal{A}_k ; but more importantly for our purposes it guarantees that the linear system arising from

any Galerkin method of approximation of (6) is invertible, and, via Céa's lemma, implies explicit error estimates for the Galerkin method solution, as discussed below.

For both formulations the following lemma holds provided Ω is Lipschitz and provided $|\eta| \leq Ck$ in the standard formulation (we shall assume henceforth that this condition always holds). Here and for the remainder of this paper $C > 0$ denotes a constant whose value may change from one occurrence to the next, but which is always independent of k , although it may (possibly) be dependent on Ω .

Lemma 21 [13, Theorem 3.6], [36, Theorem 4.2] *Assume that Ω is a bounded Lipschitz domain and $k_0 > 0$. In the case $\mathcal{A} = \mathcal{A}_{k,\eta}$ assume additionally that $|\eta| \leq Ck$. Then for both $\mathcal{A} = \mathcal{A}_k$ and $\mathcal{A} = \mathcal{A}_{k,\eta}$ there exists a constant $C_0 > 0$, independent of k , such that*

$$\|\mathcal{A}\|_{L^2(\Gamma)} \leq C_0 k^{1/2}, \quad k \geq k_0.$$

Lemma 21 suggests at worst mild growth in $\|\mathcal{A}\|_{L^2(\Gamma)}$ for both formulations as k increases. For the case $\mathcal{A} = \mathcal{A}_{k,\eta}$, with η proportional to k , it is shown in [13, 5] that $\|\mathcal{A}\|_{L^2(\Gamma)}$ does grow proportionally to $k^{1/2}$ for a polygonal scatterer, i.e. for this case at least it is known that the bound is sharp.

As alluded to above, in certain cases \mathcal{A} also satisfies the following assumptions:

Assumption 22 *There exist constants $C_1 > 0$, $\beta_1 \geq 0$, and $k_1 > 0$, independent of k , such that*

$$\|\mathcal{A}^{-1}\|_{L^2(\Gamma)} \leq C_1 k^{\beta_1}, \quad k \geq k_1,$$

Assumption 23 (Coercivity) *There exist constants $C_2 > 0$, $\beta_2 \geq 0$ and $k_2 > 0$, independent of k , such that (where $\langle \cdot, \cdot \rangle_{L^2(\Gamma)}$ denotes the inner product in $L^2(\Gamma)$)*

$$\left| \langle \mathcal{A}\psi, \psi \rangle_{L^2(\Gamma)} \right| \geq C_2 k^{-\beta_2} \|\psi\|_{L^2(\Gamma)}^2, \quad \psi \in L^2(\Gamma), \quad k \geq k_2.$$

It is a consequence of the standard Lax-Milgram lemma that, if Assumption 23 holds, then so does Assumption 22, moreover with $k_1 = k_2$, $\beta_1 = \beta_2$ and $C_1 = C_2^{-1}$.

For the standard formulation, $\mathcal{A} = \mathcal{A}_{k,\eta}$, Assumption 22 has been shown to hold for all $k_1 > 0$ if Ω is star-like and η is proportional to k ; moreover the assumption holds with $\beta_1 = 0$ so that $\|\mathcal{A}^{-1}\|_{L^2(\Gamma)}$ is bounded as $k \rightarrow \infty$ [19]. The main achievement of [36] is to show, via Morawetz-Ludwig identities, that, for the star-combined formulation $\mathcal{A} = \mathcal{A}_k$, Assumption 23 (and hence Assumption 22) holds (for Ω star-like) with $\beta_2 = 0$ for all $k_2 > 0$, moreover with the explicit formula

$$C_2 = \frac{1}{2} \operatorname{ess\,inf}_{\mathbf{x} \in \Gamma} (\mathbf{x} \cdot \mathbf{n}(\mathbf{x})).$$

By contrast, Assumption 23 has only been proven to hold for the standard combined potential operator $\mathcal{A} = \mathcal{A}_{k,\eta}$ for the special case that the scatterer is circular [23, 36] and, for k sufficiently large, for the case that the scatterer is a strictly convex C^3 domain with strictly positive curvature [14, Theorem 5.25]. However, recent 2D numerical evidence, based on clever numerical computations of coercivity constants, suggests it holds much more generally, in particular that it holds with $\beta_2 = 0$ for all star-like obstacles, and for some ‘‘non-trapping’’ non-star-like polygons (e.g. both of the examples in Figure 2) [6, Conjecture 6.2].

3 Regularity of Solutions

Our goal is to derive a numerical method for the solution of the BIE (6) (and hence of the scattering problem), whose performance does not deteriorate significantly as the wavenumber k (which is proportional to frequency) increases, equivalently as the wavelength $\lambda := 2\pi/k$ decreases. Specifically, we wish to avoid the requirement of conventional schemes for a fixed number of degrees of freedom per wavelength. To achieve this goal, our numerical method for solving (6) uses an approximation space (defined explicitly in §5) which is adapted to the high frequency asymptotic behaviour of the solution $\partial u/\partial \mathbf{n}$ on each of the sides of the polygon. For the case of a sound-soft convex polygon, this behaviour was determined in [28, 16]. A key contribution of this paper is to introduce new methods of argument which enable us to deduce precisely and rigorously this behaviour for a range of cases when the polygon is not convex.

At present our full analysis applies only to a particular class of polygons, defined below. This class includes all convex polygons, but also a large set of nonconvex star-like and non-star-like polygons.

Definition 31 *Let \mathcal{C} denote the class of all polygons $\Omega \subset \mathbb{R}^2$ for which the following two conditions are satisfied:*

1. *Each external angle is either greater than π or equal to $\pi/2$.*
2. *For each external angle equal to $\pi/2$, if Ω is rotated into the configuration in Figure 2(a), then Ω is contained entirely in the region bounded by the sides Γ_{nc} and Γ'_{nc} and the two dotted lines.*

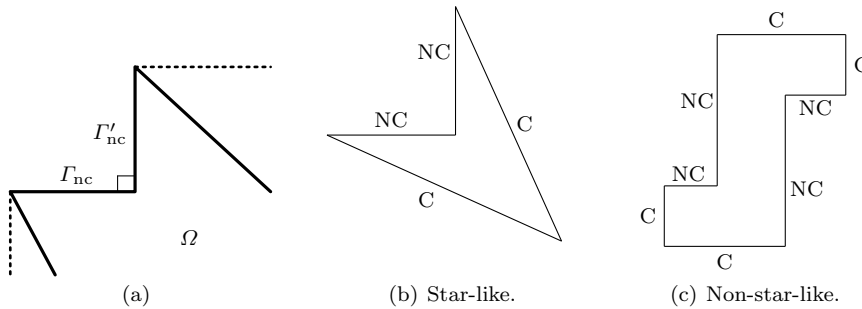


Fig. 2 (a) Illustration of condition 2 in Definition 31; (b)-(c) examples of polygonal scatterers in the class \mathcal{C} , with convex (C) and nonconvex (NC) sides labelled.

In Figure 2(b)-(c) we show two examples of members of the class \mathcal{C} , one star-like and one non-star-like. These illustrate that the class \mathcal{C} is large, but of course it is only a small subset of the set of all nonconvex polygons. The restriction in this paper to nonconvex obstacles satisfying Definition 31 is made with two points in mind.

Firstly, the constraints in this definition simplify the analysis considerably, though we shall see that this is still involved, and needs new ideas compared to

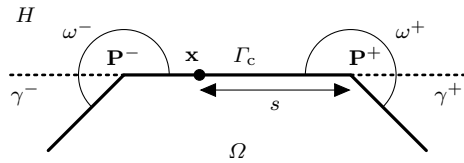


Fig. 3 Geometry of a typical convex side Γ_c .

the convex case [28]. A significant part of our analysis is achieved via explicit computations using the Green's function for a quarter-plane given by (15). Allowing an exterior angle $\omega \in (0, \pi)$ different from $\pi/2$ would require corresponding computations with the Green's function for a wedge of exterior angle ω . This extension is thus relatively straightforward if $\omega = \pi/m$, for some integer $m \geq 3$, when a method of images representation applies, more complicated otherwise. The second constraint in the above definition implies that, from each point $\mathbf{x} \in \Gamma$, at most three corners of Γ are visible. This constraint limits the complexity of the high frequency behaviour of the solution and hence the complexity of our analysis. Notably, it avoids 'trapping' domains as discussed for example in [13, 6].

Secondly, through limiting the complexity of the solution behaviour, the constraints in Definition 31 limit the complexity of the approximation space required and hence that of the algorithm; the approximation space we propose is designed having precisely the class of obstacles \mathcal{C} in mind, and cannot be expected to work more effectively than standard boundary element methods for general nonconvex polygons. Having said this, we suspect that the algorithm can easily be modified to work well for relaxation of the first constraint, allowing more general exterior angles in $(0, \pi)$ than $\pi/2$. But we think that significant algorithmic modifications would be needed to enable significant relaxation of the second constraint. We leave further discussion to future work, building on the algorithm and analysis in this paper.

For a polygon in the class \mathcal{C} we define two types of side: if the external angles at the endpoints of the side are both greater than π then we say that it is a "convex" side; if one is equal to $\pi/2$ then we say that it is a "nonconvex" side; note that nonconvex sides come in pairs. We say that a convex side is illuminated by the incident wave if $\mathbf{d} \cdot \mathbf{n} < 0$ on the side, and is in shadow if $\mathbf{d} \cdot \mathbf{n} \geq 0$.

3.1 Behaviour on convex sides

We first consider the behaviour on a typical convex side, which we denote Γ_c . As illustrated in Figure 3, we let \mathbf{P}^\pm denote the endpoints of Γ_c , and $\omega^\pm \in (\pi, 2\pi)$ the corresponding exterior angles. A point \mathbf{x} on Γ_c is then given in terms of the arc length s measured from \mathbf{P}^+ by $\mathbf{x}(s) = \mathbf{P}^+ + (s/L_c)(\mathbf{P}^- - \mathbf{P}^+)$ for $s \in [0, L_c]$, where $L_c = |\mathbf{P}^- - \mathbf{P}^+|$ is the length of Γ_c . The analysis for convex polygons in [28, 16] carries over virtually verbatim to this case. Precisely, arguing as in [28, §3], we have:

Theorem 32 *On a convex side Γ_c the representation*

$$\frac{\partial u}{\partial \mathbf{n}}(\mathbf{x}(s)) = \Psi(\mathbf{x}(s)) + v^+(s)e^{iks} + v^-(L_c - s)e^{-iks}, \quad s \in [0, L_c], \quad (9)$$

holds, where

- (i) $\Psi := 2\partial u^i/\partial \mathbf{n}$ if Γ_c is illuminated and $\Psi := 0$ otherwise;
- (ii) the functions $v^\pm(s)$ are analytic in the right half-plane $\operatorname{Re}[s] > 0$; further, for every $k_0 > 0$ we have

$$|v^\pm(s)| \leq \begin{cases} CM(u)k|ks|^{-\delta^\pm}, & 0 < |s| \leq 1/k, \\ CM(u)k|ks|^{-1/2}, & |s| > 1/k, \end{cases} \quad \operatorname{Re}[s] > 0, \quad (10)$$

for $k \geq k_0$, where $\delta^\pm := 1 - \pi/\omega^\pm \in (0, 1/2)$ and

$$M(u) := \sup_{\mathbf{x} \in D} |u(\mathbf{x})|. \quad (11)$$

The constant $C > 0$ depends only on Ω and k_0 .

Remark 33 *The dependence of $M(u)$ on the wavenumber k is not yet fully understood. In [28, Theorem 4.3] it is shown that $M(u) = \mathcal{O}(k^{1/2} \log^{1/2} k)$ as $k \rightarrow \infty$, uniformly with respect to the angle of incidence, when Ω is a star-like polygon. However, it is plausible that in fact $M(u) = \mathcal{O}(1)$ as $k \rightarrow \infty$ in this case, and indeed for the whole class \mathcal{C} .*

Remark 34 *The representation (9) can be interpreted in terms of high frequency asymptotics as follows. The first term, Ψ (corresponding to V_0 in (1)), is the geometrical optics (sometimes called the physical optics) approximation to $\partial u/\partial \mathbf{n}$, representing the contribution of the incident and reflected rays (where they are present). The second and third terms represent contributions due to diffracted rays emanating from the corners \mathbf{P}^+ and \mathbf{P}^- , respectively.*

3.2 Behaviour on nonconvex sides

We now consider the typical behaviour on a nonconvex side, which we denote Γ_{nc} . As illustrated in Figure 4(a), we let \mathbf{P} and \mathbf{Q} denote the endpoints of Γ_{nc} , and \mathbf{P}' and \mathbf{Q}' the endpoints of the adjoining nonconvex side, which we denote Γ'_{nc} . We let L_{nc} and L'_{nc} denote the lengths of Γ_{nc} and Γ'_{nc} , respectively, and we denote the exterior angle at \mathbf{P} by ω . A point \mathbf{x} on Γ_{nc} is then given in terms of the arc length s measured from \mathbf{Q} by $\mathbf{x}(s) = \mathbf{Q} + (s/L_{nc})(\mathbf{P} - \mathbf{Q})$ for $s \in [0, L_{nc}]$. We also introduce local Cartesian coordinates $\mathbf{x} = (x_1, x_2)$ and polar coordinates (r, θ) (both with the origin at \mathbf{P}'), as defined in Figure 4(a). We note that any nonconvex side can be transformed to this configuration by a rotation and a reflection of Ω .

We expect the high frequency asymptotic behaviour of $\partial u/\partial \mathbf{n}$ on Γ_{nc} to involve: diffracted waves from the corners \mathbf{P} and \mathbf{P}' ; reflection by the side Γ'_{nc} ; and, depending on the direction of incidence, illumination (partial or otherwise). One might expect the leading order behaviour on Γ_{nc} to be given by the canonical solution corresponding to diffraction of u^i by the infinite wedge formed by extending the two sides emanating from \mathbf{P}' towards the bottom right of Figure 4(a). In fact,

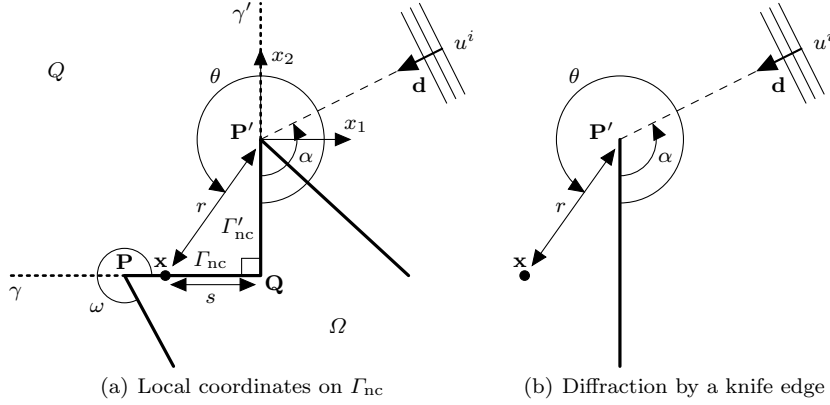


Fig. 4 Geometry of a typical nonconvex side Γ_{nc} .

the correct leading order behaviour is captured by a simpler canonical solution, namely that corresponding to diffraction of u^i by the infinite knife edge formed by extending the side Γ'_{nc} towards the bottom of Figure 4(a), as illustrated in Figure 4(b). That the leading order behaviour is the same for the two canonical problems (with the difference between the two solutions being a higher order term which varies slowly across the shadow boundary), is discussed in detail in [34].

Lemma 35 ([8, §8.2]) *Let (r, θ) be polar coordinates with $r \in [0, \infty)$ and $\theta \in [0, 2\pi)$. Let u^d denote the solution to the problem of diffraction of the plane wave $u^i = e^{ik\mathbf{x}\cdot\mathbf{d}}$ by the infinite knife edge $\{(r, 0) : r \in [0, \infty)\}$ with Dirichlet boundary conditions. If $\theta = \alpha$ is the direction from which the incident wave arrives (as in Figure 4(b)), then*

$$u^d(r, \theta, \alpha) = E(r, \theta - \alpha) - E(r, \theta + \alpha),$$

where $E(r, \psi) = e^{-ikr \cos \psi} \text{Fr}(-\sqrt{2kr} \cos(\psi/2))$, and Fr is a Fresnel integral, defined by $\text{Fr}(\mu) = (e^{-i\pi/4}/\sqrt{\pi}) \int_{\mu}^{\infty} e^{iz^2} dz$.

The key result that we require for the design of our approximation space is the following theorem, which we prove in §4.

Theorem 36 *Suppose that Assumption 22 holds. Then on the nonconvex side Γ_{nc} the representation*

$$\frac{\partial u}{\partial \mathbf{n}}(\mathbf{x}(s)) = \Psi(\mathbf{x}(s)) + v^+(L_{\text{nc}} + s)e^{iks} + v^-(L_{\text{nc}} - s)e^{-iks} + v(s)e^{ikr}, \quad s \in [0, L_{\text{nc}}], \quad (12)$$

holds, where $r = r(s) = \sqrt{s^2 + L_{\text{nc}}^2}$ and

- (i) $\Psi := 2\partial u^d/\partial \mathbf{n}$ if $\pi/2 \leq \alpha \leq 3\pi/2$, and $\Psi := 0$ otherwise;
- (ii) the functions $v^{\pm}(s)$ are analytic in $\text{Re}[s] > 0$; further, for every $k_0 > 0$ they satisfy the bounds (10) for $k \geq k_0$, with $\delta^{\pm} = 1 - \pi/\omega \in (0, 1/2)$ and $C > 0$ depending only on Ω and k_0 ;

(iii) the function $v(s)$ is analytic in the k -independent complex neighbourhood $D_\varepsilon := \{s \in \mathbb{C} : \text{dist}(s, [0, L_{\text{nc}}]) < \varepsilon\}$ of $[0, L_{\text{nc}}]$, where

$$\varepsilon := L'_{\text{nc}}/(32\sqrt{2}); \quad (13)$$

further

$$|v(s)| \leq CC_1 k^{1+\beta_1} \log^{1/2}(2+k), \quad s \in D_\varepsilon, k \geq k_1, \quad (14)$$

where β_1 , k_1 , and C_1 are the constants from Assumption 22 and $C > 0$ depends only on Ω and k_1 .

Remark 37 The representation (12) can be interpreted in terms of high frequency asymptotics as follows. The first term, Ψ , represents the leading order high frequency behaviour due to the diffraction of the incident wave by the corner \mathbf{P}' ; depending on the value of α , this includes contributions from the incident wave, the reflection of the incident wave in Γ'_{nc} , and the associated shadow boundary behaviour. The final term represents an additional contribution associated with diffracted rays emanating from the corner \mathbf{P}' . The third term represents the contribution due to diffracted rays emanating from the corner \mathbf{P} , and the second term represents the contribution due to ‘reflected-diffracted’ rays emanating from the corner \mathbf{P} and reflected at \mathbf{Q} .

As alluded to above (details follow in §5), our numerical method uses an approximation space based on the representations (9) and (12), in which the factors v^\pm and v are approximated by piecewise polynomials, rather than approximating $\partial u/\partial \mathbf{n}$ itself as in conventional methods. The advantage of our approach is that the functions v^\pm and v are non-oscillatory (as quantified in Theorems 32 and 36), and can therefore be approximated much more efficiently than $\partial u/\partial \mathbf{n}$.

4 Proof of Theorem 36

We begin by outlining the structure of the proof of Theorem 36. To that end we first summarise the proof of the regularity result for a convex side, Theorem 32, following the arguments of [28, 16]. There the key first step was to apply Green’s representation theorem in the half plane $H \subset D$ whose boundary extends the side Γ_c , as illustrated in Figure 3. The Dirichlet Green’s function for this domain is known explicitly by the method of images in terms of the fundamental solution Φ_k . This gives $\partial u/\partial \mathbf{n}$ on Γ_c as a leading order term, plus the sum of two integrals over the contours γ^\pm . The integrand in the integral over γ^\pm contains u restricted to γ^\pm as a factor, and the integrals over γ^+ and γ^- correspond to the diffracted fields emanating from the corners \mathbf{P}^+ and \mathbf{P}^- , respectively. This motivates extracting out as factors the respective phases e^{iks} and e^{-iks} from these integrals, leaving the factors $v^+(s)$ and $v^-(L_c - s)$ in (9). Finally, using analyticity properties of the Hankel function that appears in the definition of Φ_k , it can be shown that the functions $v^\pm(s)$ can be analytically continued into the complex plane where they satisfy the bounds (10) (see [28, Theorem 3.2]).

On the nonconvex side Γ_{nc} we adopt a similar methodology. However, we now apply (in Lemma 41) Green’s representation theorem in the quarter plane Q whose boundary extends the sides Γ_{nc} and Γ'_{nc} , as illustrated in Figure 4(a). Again, the

Dirichlet Green's function for this domain is known explicitly (see (15)) by the method of images. (This simple representation for the Green's function simplifies the calculations throughout this section; it is this which motivates the requirement in Definition 31 that the exterior angles less than π are exactly $\pi/2$.) This gives $\partial u/\partial \mathbf{n}$ on Γ_{nc} as a leading order term, plus the sum of integrals over the contours γ and γ' ; these integrals contain u restricted to γ or γ' as a factor (see (21)).

We expect the integral over γ to correspond to the field diffracted at \mathbf{P} , and its subsequent reflection at \mathbf{Q} . In fact, this integral can be analysed in exactly the same way as for a convex side, as described above, and gives rise to the terms $v^+(L_{\text{nc}} + s)e^{iks}$ and $v^-(L_{\text{nc}} - s)e^{-iks}$ in the representation (12). The remaining terms in (12) arise from the integral over γ' , which we expect to correspond to the field diffracted at \mathbf{P}' .

To analyse this integral we split it further, using the fact that $u = u^i + u^s$. We consider the contribution from u^s in Lemma 43, where we extract as a factor the expected phase e^{ikr} and show that the remaining function $W^s(s)$ can be analytically continued into the complex plane. This is more complicated than the corresponding arguments in the convex case. First we need to substitute for u^s using the representation theorem (5), which gives, after an application of Fubini's theorem, the representation (25) as an integral around Γ involving $\partial u/\partial \mathbf{n}$. The next task is to show that $K(\cdot, \mathbf{z})$ in the integrand, given as the integral (26) along γ' , has an analytic continuation into a (\mathbf{z} - and k -independent) neighbourhood of $[0, L_{\text{nc}}]$, and to bound $K(\cdot, \mathbf{z})$ in this neighbourhood for $\mathbf{z} \in \Gamma$ (Lemma 45). To achieve this aim it is convenient first to show that one can deform the contour of integration γ' in (26) to a contour on which the integrand decays exponentially, obtaining the representation (36). To show these results we require auxiliary results, Lemmas 44, 46, and 47. In a final step we bound $W^s(s)$ in the complex plane via the application (47) of the Cauchy-Schwarz inequality, bounding $\|\partial u/\partial \mathbf{n}\|_{L^2(\Gamma)}$ via the integral equation (6) and the bound on $\|\mathcal{A}^{-1}\|_{L^2(\Gamma)}$ in Assumption 22. (It is precisely at this point where Assumption 22 is needed.) This proof of Lemma 43 occupies §4.1.

We consider the contribution from u^i in Lemma 42 (which is proved in §4.2), where we apply a similar (but simpler) approach, making use of the tools developed in the proof of Lemma 43. There is one complication: when $\alpha \in (\pi/2, 3\pi/2)$, in which case Γ_{nc} is partially (or fully) illuminated by the incident wave, we first have to subtract off the canonical solution u^d from u^i . The analysis is completed by applying Green's representation theorem for u^d in the half-plane $x_1 < 0$ (Proposition 48).

We thus begin our proof of Theorem 36 by deriving a representation formula for u in the quarter-plane whose boundary contains the sides Γ'_{nc} and Γ_{nc} . Let $\gamma := \{(x_1, -L'_{\text{nc}}) : x_1 < -L_{\text{nc}}\}$ and $\gamma' := \{(0, x_2) : x_2 > 0\}$ denote the extensions of Γ_{nc} and Γ'_{nc} , respectively (see Figure 4(a)). Then $\partial Q := \gamma \cup \Gamma_{\text{nc}} \cup \Gamma'_{\text{nc}} \cup \gamma'$ is the boundary of the quarter-plane $Q := \{(x_1, x_2) : x_1 < 0, x_2 > -L'_{\text{nc}}\}$ whose Dirichlet Green's function is, by the method of images,

$$G_k(\mathbf{x}, \mathbf{y}) := \Phi_k(\mathbf{x}, \mathbf{y}) - \Phi_k(\mathbf{x}, \mathbf{y}^*) - \Phi_k(\mathbf{x}, \mathbf{y}') + \Phi_k(\mathbf{x}, \mathbf{y}^{*'}), \quad (15)$$

where $*$ and $'$ are operations of reflection in the lines $\gamma \cup \Gamma_{\text{nc}}$ and $\Gamma'_{\text{nc}} \cup \gamma'$, respectively. For reference, the incident wave and its reflections in the extensions of

these lines (assuming a sound-soft boundary condition (4)) are given explicitly by

$$\begin{aligned} u^i(\mathbf{x}) &= \exp(ik(-x_1 \sin \alpha + x_2 \cos \alpha)), \\ (u^i)^*(\mathbf{x}) &= -\exp(ik(-x_1 \sin \alpha - (x_2 + 2L'_{\text{nc}}) \cos \alpha)), \\ (u^i)'(\mathbf{x}) &= -\exp(ik(x_1 \sin \alpha + x_2 \cos \alpha)), \\ (u^i)^{*\prime}(\mathbf{x}) &= \exp(ik(x_1 \sin \alpha - (x_2 + 2L'_{\text{nc}}) \cos \alpha)). \end{aligned}$$

We also recall that \mathbf{n} is the unit normal directed into D , i.e. into the interior of Q .

We then have the following representation formulae:

Lemma 41 (i) $u^s(\mathbf{x}) = \int_{\partial Q} \frac{\partial G_k(\mathbf{x}, \mathbf{y})}{\partial \mathbf{n}(\mathbf{y})} u^s(\mathbf{y}) \, ds(\mathbf{y}), \quad \mathbf{x} \in Q; \quad (16)$

(ii) $u^i(\mathbf{x}) = \Psi_1(\mathbf{x}) + \int_{\partial Q} \frac{\partial G_k(\mathbf{x}, \mathbf{y})}{\partial \mathbf{n}(\mathbf{y})} u^i(\mathbf{y}) \, ds(\mathbf{y}), \quad \mathbf{x} \in Q, \quad (17)$

where, for $\pi \leq \alpha \leq 3\pi/2$,

$$\begin{aligned} \Psi_1(\mathbf{x}) &:= u^i(\mathbf{x}) + (u^i)^*(\mathbf{x}) + (u^i)'(\mathbf{x}) + (u^i)^{*\prime}(\mathbf{x}) \\ &= 4 \exp(-ikL'_{\text{nc}} \cos \alpha) \sin(kx_1 \sin \alpha) \sin(k(x_2 + L'_{\text{nc}}) \cos \alpha), \end{aligned}$$

while $\Psi_1(\mathbf{x}) := 0$, otherwise;

(iii) $u(\mathbf{x}) = \Psi_1(\mathbf{x}) + \int_{\gamma \cup \gamma'} \frac{\partial G_k(\mathbf{x}, \mathbf{y})}{\partial \mathbf{n}(\mathbf{y})} u(\mathbf{y}) \, ds(\mathbf{y}), \quad \mathbf{x} \in Q.$

Proof (i) For $R > 0$ define $Q_R := \{\mathbf{y} \in Q : |\mathbf{y}| < R\}$, with boundary ∂Q_R . Applying Green's theorem and Green's representation theorem [14, Theorems 2.19, 2.20] gives that

$$u^s(\mathbf{x}) = \int_{\partial Q_R} \left(\frac{\partial G_k(\mathbf{x}, \mathbf{y})}{\partial \mathbf{n}(\mathbf{y})} u^s(\mathbf{y}) - G_k(\mathbf{x}, \mathbf{y}) \frac{\partial u^s}{\partial \mathbf{n}}(\mathbf{y}) \right) ds(\mathbf{y}), \quad \mathbf{x} \in Q_R, \quad (18)$$

where the normal \mathbf{n} is directed into the interior of Q_R . Then, since $G_k(\mathbf{x}, \mathbf{y}) = 0$ on ∂Q and both $G_k(\mathbf{x}, \cdot)$ and u^s satisfy the Sommerfeld radiation condition, (16) is obtained from (18) by taking the limit $R \rightarrow \infty$ (see, e.g., [21, Theorem 3.3]).

(ii) For $R > 0$ define $\mathbf{x}_R := -R\mathbf{d} = R(\sin \alpha, -\cos \alpha)$, and $u_R^i(\mathbf{x}) := C_R \Phi_k(\mathbf{x}, \mathbf{x}_R)$, where $C_R := e^{-i\pi/4} \sqrt{8\pi k R} e^{-ikR}$. Note that, for fixed R , $u_R^i(\mathbf{x})$ satisfies the Sommerfeld radiation condition as $|\mathbf{x}| \rightarrow \infty$, but, for fixed \mathbf{x} , $u_R^i(\mathbf{x}) \rightarrow u^i(\mathbf{x})$ as $R \rightarrow \infty$. If $\alpha \notin [\pi, 3\pi/2]$, then $u_R^i(\mathbf{x})$ is regular throughout Q , and, arguing as in part (i),

$$u_R^i(\mathbf{x}) = \int_{\partial Q} \frac{\partial G_k(\mathbf{x}, \mathbf{y})}{\partial \mathbf{n}(\mathbf{y})} u_R^i(\mathbf{y}) \, ds(\mathbf{y}), \quad \mathbf{x} \in Q. \quad (19)$$

If $\alpha \in (\pi, 3\pi/2)$, $u_R^i(\mathbf{x})$ is singular at $\mathbf{x} = \mathbf{x}_R \in Q$, and (19) must be modified to

$$u_R^i(\mathbf{x}) = C_R G_k(\mathbf{x}, \mathbf{x}_R) + \int_{\partial Q} \frac{\partial G_k(\mathbf{x}, \mathbf{y})}{\partial \mathbf{n}(\mathbf{y})} u_R^i(\mathbf{y}) \, ds(\mathbf{y}), \quad \mathbf{x} \in Q, \mathbf{x} \neq \mathbf{x}_R. \quad (20)$$

By the dominated convergence theorem, formula (17) is then obtained by letting $R \rightarrow \infty$ in (19) and (20), since, for fixed \mathbf{x} , $C_R G_k(\mathbf{x}, \mathbf{x}_R)$ tends to $u^i(\mathbf{x}) + (u^i)^*(\mathbf{x}) + (u^i)'(\mathbf{x}) + (u^i)^{*\prime}(\mathbf{x})$ as $R \rightarrow \infty$. The result for $\alpha = \pi$ and $3\pi/2$ follows by taking the limits $\alpha \rightarrow \pi$ and $\alpha \rightarrow 3\pi/2$ in (17).

(iii) This is a trivial consequence of (i) and (ii) and the fact that $u = 0$ on Γ .

As a consequence of Lemma 41(iii) we have that

$$\frac{\partial u}{\partial \mathbf{n}}(\mathbf{x}) = \frac{\partial \Psi_1}{\partial \mathbf{n}}(\mathbf{x}) + \int_{\gamma \cup \gamma'} \frac{\partial^2 G_k(\mathbf{x}, \mathbf{y})}{\partial \mathbf{n}(\mathbf{x}) \partial \mathbf{n}(\mathbf{y})} u(\mathbf{y}) \, ds(\mathbf{y}), \quad \mathbf{x} \in \Gamma_{\text{nc}}. \quad (21)$$

Theorem 36 follows from a careful analysis of the integral in (21). The terms $v^+(L_{\text{nc}} + s)e^{iks}$ and $v^-(L_{\text{nc}} - s)e^{-iks}$ in the representation (12) arise from the integral over γ . Indeed, noting that

$$\frac{\partial^2 G_k(\mathbf{x}, \mathbf{y})}{\partial \mathbf{n}(\mathbf{x}) \partial \mathbf{n}(\mathbf{y})} = 2 \frac{\partial^2 \Phi_k(\mathbf{x}, \mathbf{y})}{\partial \mathbf{n}(\mathbf{x}) \partial \mathbf{n}(\mathbf{y})} - 2 \frac{\partial^2 \Phi_k(\mathbf{x}, \mathbf{y}')}{\partial \mathbf{n}(\mathbf{x}) \partial \mathbf{n}(\mathbf{y})}, \quad \mathbf{x} \in \Gamma_{\text{nc}}, \mathbf{y} \in \gamma,$$

where $\mathbf{y}' := (-y_1, y_2)$, we find that, for $\mathbf{x} \in \Gamma_{\text{nc}}$,

$$\int_{\gamma} \frac{\partial^2 G_k(\mathbf{x}, \mathbf{y})}{\partial \mathbf{n}(\mathbf{x}) \partial \mathbf{n}(\mathbf{y})} u(\mathbf{y}) \, ds(\mathbf{y}) = 2 \int_{\gamma} \frac{\partial^2 \Phi_k(\mathbf{x}, \mathbf{y})}{\partial \mathbf{n}(\mathbf{x}) \partial \mathbf{n}(\mathbf{y})} u(\mathbf{y}) \, ds(\mathbf{y}) - 2 \int_{\tilde{\gamma}} \frac{\partial^2 \Phi_k(\mathbf{x}, \mathbf{y})}{\partial \mathbf{n}(\mathbf{x}) \partial \mathbf{n}(\mathbf{y})} u(\mathbf{y}') \, ds(\mathbf{y}), \quad (22)$$

with $\tilde{\gamma} := \{(x_1, -L'_{\text{nc}}) : x_1 > L_{\text{nc}}\}$. This expression is very similar to that encountered in the derivation of the regularity results on a convex side. Indeed, arguing almost exactly as in [28, §3] (and see also [16, §3]), it can be shown from (22) that

$$\int_{\gamma} \frac{\partial^2 G_k(\mathbf{x}, \mathbf{y})}{\partial \mathbf{n}(\mathbf{x}) \partial \mathbf{n}(\mathbf{y})} u(\mathbf{y}) \, ds(\mathbf{y}) = v^-(L_{\text{nc}} - s)e^{-iks} + v^+(L_{\text{nc}} + s)e^{iks}, \quad \mathbf{x}(s) \in \Gamma_{\text{nc}},$$

where $v^{\pm}(s)$ are analytic in $\text{Re}[s] > 0$, where they satisfy the bounds (10) with $\delta^{\pm} = 1 - \pi/\omega$. This is the assertion in paragraph (ii) of Theorem 36.

We now consider the integral over γ' in (21). Noting that

$$\frac{\partial^2 G_k(\mathbf{x}, \mathbf{y})}{\partial \mathbf{n}(\mathbf{x}) \partial \mathbf{n}(\mathbf{y})} = -4 \frac{\partial^2 \Phi_k(\mathbf{x}, \mathbf{y})}{\partial x_2 \partial y_1}, \quad \mathbf{x} \in \Gamma_{\text{nc}}, \mathbf{y} \in \gamma',$$

and using the decomposition $u = u^i + u^s$, we have, for $\mathbf{x} \in \Gamma_{\text{nc}}$, that

$$\int_{\gamma'} \frac{\partial^2 G_k(\mathbf{x}, \mathbf{y})}{\partial \mathbf{n}(\mathbf{x}) \partial \mathbf{n}(\mathbf{y})} u(\mathbf{y}) \, ds(\mathbf{y}) = -4 \int_{\gamma'} \frac{\partial^2 \Phi_k(\mathbf{x}, \mathbf{y})}{\partial x_2 \partial y_1} u^i(\mathbf{y}) \, ds(\mathbf{y}) - 4 \int_{\gamma'} \frac{\partial^2 \Phi_k(\mathbf{x}, \mathbf{y})}{\partial x_2 \partial y_1} u^s(\mathbf{y}) \, ds(\mathbf{y}). \quad (23)$$

The assertions in paragraphs (i) and (iii) of Theorem 36 then follow from (21), (23) and Lemmas 42 and 43 below.

Lemma 42 For $\mathbf{x} = (-s, -L'_{\text{nc}}) \in \Gamma_{\text{nc}}$,

$$-4 \int_{\gamma'} \frac{\partial^2 \Phi_k(\mathbf{x}, \mathbf{y})}{\partial x_2 \partial y_1} u^i(\mathbf{y}) \, ds(\mathbf{y}) = \Psi(\mathbf{x}) - \frac{\partial \Psi_1}{\partial \mathbf{n}}(\mathbf{x}) + e^{ikr} W^i(s),$$

where $W^i(s)$ is analytic in D_{ε} , with ε given by (13); further, for every $k_0 > 0$,

$$\left| W^i(s) \right| \leq C k^{1/2}, \quad s \in D_{\varepsilon}, k \geq k_0,$$

where $C > 0$ depends only on Ω and k_0 .

Lemma 43 *If Assumption 22 holds, then, for $\mathbf{x} = (-s, -L'_{\text{nc}}) \in \Gamma_{\text{nc}}$,*

$$-4 \int_{\gamma'} \frac{\partial^2 \Phi_k(\mathbf{x}, \mathbf{y})}{\partial x_2 \partial y_1} u^s(\mathbf{y}) \, ds(\mathbf{y}) = e^{ikr} W^s(s),$$

where $W^s(s)$ is analytic in D_ε , with ε given by (13); further, where β_1 , k_1 and C_1 are the constants in Assumption 22,

$$|W^s(s)| \leq CC_1 k^{1+\beta_1} \log^{1/2}(2+k), \quad s \in D_\varepsilon, k \geq k_1, \quad (24)$$

where $C > 0$ depends only on Ω and k_1 .

We begin by proving Lemma 43. Some of the results needed for this proof will be used again in the proof of Lemma 42.

4.1 Proof of Lemma 43

For $\mathbf{x} = (-s, -L'_{\text{nc}}) \in \Gamma_{\text{nc}}$ we have $r = r(s) = \sqrt{s^2 + L'^2_{\text{nc}}}$. Thus, to prove the lemma we have to show that

$$W^s(s) := -4 \exp\left(-ik\sqrt{s^2 + L'^2_{\text{nc}}}\right) \int_{\gamma'} \frac{\partial^2 \Phi_k(\mathbf{x}, \mathbf{y})}{\partial x_2 \partial y_1} u^s(\mathbf{y}) \, ds(\mathbf{y})$$

is analytic in D_ε , satisfying the bound (24). Substituting for u^s using (5), and switching the order of integration, justified by Fubini's theorem, gives

$$W^s(s) = \int_\Gamma K(s, \mathbf{z}) \frac{\partial u}{\partial \mathbf{n}}(\mathbf{z}) \, ds(\mathbf{z}), \quad (25)$$

where, for $s \in \mathbb{R}$ and $\mathbf{z} \in \Gamma$,

$$K(s, \mathbf{z}) := 4 \exp\left(-ik\sqrt{s^2 + L'^2_{\text{nc}}}\right) \int_0^\infty \frac{\partial^2 \Phi_k((-s, -L'_{\text{nc}}), (0, y_2))}{\partial x_2 \partial y_1} \Phi_k((0, y_2), \mathbf{z}) \, dy_2, \quad (26)$$

and, by the recurrence and differentiation formulae for Hankel functions [1, §10.6],

$$\begin{aligned} \Phi_k((0, y_2), \mathbf{z}) &= \frac{i}{4} H_0^{(1)}\left(k\sqrt{z_1^2 + (y_2 - z_2)^2}\right), \\ \frac{\partial^2 \Phi_k((-s, -L'_{\text{nc}}), (0, y_2))}{\partial x_2 \partial y_1} &= -\frac{ik^2 s(L'_{\text{nc}} + y_2)}{4(s^2 + (L'_{\text{nc}} + y_2)^2)} H_2^{(1)}\left(k\sqrt{s^2 + (L'_{\text{nc}} + y_2)^2}\right). \end{aligned}$$

We recall that $H_n^{(1)}(z)$ is analytic in $|z| > 0$, $|\arg(z)| < \pi$. To derive bounds on $K(s, \mathbf{z})$ we need bounds on $H_n^*(z) := e^{-iz} H_n^{(1)}(z)$. From [1, §10.2(ii), §10.17.5] it follows that, for some constant $C > 0$,

$$|H_0^*(z)| \leq C|z|^{-1/2}, \quad |z| > 0, \quad |\arg(z)| \leq \pi/2 \quad (27)$$

and that, for every $c > 0$ there exists $C > 0$ such that

$$|H_2^*(z)| \leq C|z|^{-1/2}, \quad |z| > c, \quad |\arg(z)| \leq \pi/2. \quad (28)$$

Note that, for $s \in \mathbb{R}$ and $\mathbf{z} \in \Gamma$,

$$K(s, \mathbf{z}) = \int_0^\infty e^{ik\phi(s, y_2, \mathbf{z})} S_k(s, y_2, \mathbf{z}) dy_2, \quad (29)$$

where $\phi(s, y_2, \mathbf{z}) := \chi(s, L'_{\text{nc}}, y_2) - \chi(s, L'_{\text{nc}}, 0) + \chi(z_1, -z_2, y_2)$ and

$$S_k(s, y_2, \mathbf{z}) := -\frac{k^2 s(L'_{\text{nc}} + y_2)}{4(\chi(s, L'_{\text{nc}}, y_2))^2} H_2^*(k\chi(s, L'_{\text{nc}}, y_2)) H_0^*(k\chi(z_1, -z_2, y_2)),$$

with $\chi(a, b, c) := \sqrt{a^2 + (b+c)^2}$. We present some elementary properties of $\chi(a, b, c)$, required below, in the following lemma.

Lemma 44 *Let $a, b \in \mathbb{R}$, and let $\chi(a, b, c) := \sqrt{a^2 + (b+c)^2}$, for $c \in \mathbb{C}$, taking the principal value for the square root. Then:*

(i) $\chi(a, b, c)$ is analytic in the complex variable c in the half-plane $\text{Re}[c] > -b$, with

$$\text{Re}[\chi(a, b, c)] \geq \text{Re}[c] + b > 0 \quad (30)$$

and

$$\text{Im}[\chi(a, b, c)] \geq 0, \quad \text{if } \text{Im}[c] \geq 0; \quad (31)$$

(ii) in particular, for $b > 0$ and $t \geq 0$ we have

$$\text{Re}[\chi(a, b, te^{i\pi/4})] \geq \frac{\sqrt{a^2 + b^2} + t}{2} \quad (32)$$

and

$$\text{Im}[\chi(a, b, te^{i\pi/4})] \geq \frac{bt}{\sqrt{2}\sqrt{a^2 + b^2}}. \quad (33)$$

Proof Write $c = c_r + ic_i$ where $c_r > -b$, $c_i \in \mathbb{R}$. Then $a^2 + (b+c)^2 = \xi + i\eta$, where $\xi := a^2 + (b+c_r)^2 - c_i^2$, $\eta := 2c_i(b+c_r)$. For (i), it follows from $c_r > -b$ that $\eta \neq 0$, unless $c_i = 0$, in which case $\xi > 0$. So $\chi(a, b, c)$ is analytic in $\text{Re}[c] > -b$ with

$$\text{Re}[\chi(a, b, c)] = \sqrt{\frac{\xi + (\xi^2 + \eta^2)^{1/2}}{2}} > 0, \quad (34)$$

$$\text{Im}[\chi(a, b, c)] = \text{sgn}(c_i) \sqrt{\frac{-\xi + (\xi^2 + \eta^2)^{1/2}}{2}}, \quad (35)$$

which gives (31). Writing

$$2\text{Re}[\chi(a, b, c)]^2 = 2(b+c_r)^2 + \mu_1,$$

where $\mu_1 := \sqrt{(a^2 - c_i^2 + (b+c_r)^2)^2 + 4c_i^2(b+c_r)^2} + a^2 - c_i^2 - (b+c_r)^2$, and noting that

$$(a^2 - c_i^2 + (b+c_r)^2)^2 + 4c_i^2(b+c_r)^2 - (a^2 - c_i^2 - (b+c_r)^2)^2 = 4a^2(b+c_r)^2 \geq 0,$$

it follows that $\mu_1 \geq 0$, and hence (30) holds.

For (ii), note that, when $c = te^{i\pi/4}$ with $t \geq 0$, we have $\xi = a^2 + b^2 + \sqrt{2}bt \geq a^2 + b^2$ and $\eta = t(\sqrt{2}b + t) \geq t^2$, and (32) follows from (34). Also, by (35),

$$2(a^2 + b^2) \operatorname{Im} \left[\chi(a, b, te^{i\pi/4}) \right]^2 = b^2 t^2 + \mu_2,$$

where $\mu_2 := -(b^2 t^2 + (a^2 + b^2)\xi) + (a^2 + b^2)\sqrt{\xi^2 + \eta^2}$. A little algebraic manipulation reveals that

$$(a^2 + b^2)^2(\xi^2 + \eta^2) - (b^2 t^2 + (a^2 + b^2)\xi)^2 = t^3 a^2 \left(2\sqrt{2}b(a^2 + b^2) + (a^2 + 2b^2)t \right) \geq 0.$$

Hence $\mu_2 \geq 0$ and (33) follows.

In order to prove Lemma 43 we must consider the analytic continuation of $K(s, \mathbf{z})$ into the complex s -plane. But before complexifying s it is helpful to modify the representation (29) by deforming the contour of integration off the real line. From (29) it follows from Cauchy's theorem that, for $s \in \mathbb{R}$ and $\mathbf{z} \in \Gamma$, where $f(w) := e^{ik\phi(s, w, \mathbf{z})} S_k(s, w, \mathbf{z})$,

$$K(s, \mathbf{z}) = \int_{\gamma^*} f(w) dw = e^{i\pi/4} \int_0^\infty e^{ik\phi(s, te^{i\pi/4}, \mathbf{z})} S_k(s, te^{i\pi/4}, \mathbf{z}) dt, \quad (36)$$

where $\gamma^* = \{w = te^{i\pi/4} : t \geq 0\}$. This application of Cauchy's theorem is valid since, by Lemma 44(i), $f(w)$ is analytic in $\operatorname{Re}[w] > 0$; further, $\operatorname{Im}[\phi(s, w, \mathbf{z})] \geq 0$, so that $|e^{ik\phi(s, w, \mathbf{z})}| \leq 1$, if $\operatorname{Re}[w] > 0$ and $\operatorname{Im}[w] \geq 0$; moreover, the bounds (30), (27), and (28) imply that

$$S_k(s, w, \mathbf{z}) = \mathcal{O}\left(|w|^{-1/2}\right), \quad \text{as } |w| \rightarrow 0, \quad S_k(s, w, \mathbf{z}) = \mathcal{O}\left(|w|^{-2}\right), \quad \text{as } |w| \rightarrow \infty,$$

uniformly in $\arg(w)$, for $0 \leq \arg(w) \leq \pi/4$.

Having established the validity of the representation (36) for $s \in \mathbb{R}$, we now show that this same formula represents the analytic continuation of $K(s, \mathbf{z})$.

Lemma 45 *For $\mathbf{z} \in \Gamma$, $K(s, \mathbf{z})$, defined by (36), is analytic as a function of s in D_ε , with ε given by (13). Further, for every $k_0 > 0$,*

$$|K(s, \mathbf{z})| \leq Ck^{1/2}\zeta(\mathbf{z}), \quad s \in D_\varepsilon, \quad k \geq k_0, \quad \mathbf{z} \in \Gamma, \quad (37)$$

where $C > 0$ depends only on Ω and k_0 , and

$$\zeta(\mathbf{z}) := \begin{cases} 1, & 0 < k|\mathbf{z}| < 1, \\ (k|\mathbf{z}|)^{-1/2}, & k|\mathbf{z}| \geq 1. \end{cases}$$

The proof of Lemma 45 is based on the following two intermediate results.

Lemma 46 *For $t \geq 0$ and $\mathbf{z} \in \Gamma$, $\phi(s, te^{i\pi/4}, \mathbf{z})$ is analytic as a function of s in D_ε , with ε given by (13). Further,*

$$\operatorname{Im} \left[\phi(s, te^{i\pi/4}, \mathbf{z}) \right] \geq \frac{L'_{\text{nc}} t}{2\sqrt{2}\sqrt{L_{\text{nc}}^2 + L_{\text{nc}}^2}}, \quad s \in D_\varepsilon, \quad t \geq 0, \quad \mathbf{z} \in \Gamma. \quad (38)$$

Proof Suppose $t \geq 0$ and $\mathbf{z} \in \Gamma$. For $s_0 \in [0, L_{\text{nc}}]$,

$$\text{Im} \left[\phi(s_0, te^{i\pi/4}, \mathbf{z}) \right] = \text{Im} \left[\chi(s_0, L'_{\text{nc}}, te^{i\pi/4}) \right] + \text{Im} \left[\chi(z_1, -z_2, te^{i\pi/4}) \right] \geq \frac{L'_{\text{nc}} t}{\sqrt{2} \sqrt{s_0^2 + L_{\text{nc}}'^2}}, \quad (39)$$

by (33) and (31), applied to $\chi(s_0, L'_{\text{nc}}, te^{i\pi/4})$ and $\chi(z_1, -z_2, te^{i\pi/4})$, respectively. We next note that, for $s \in \mathbb{C}$,

$$\phi(s, te^{i\pi/4}, \mathbf{z}) = \frac{A}{B(s)} + \chi(z_1, -z_2, te^{i\pi/4}),$$

where $A := te^{i\pi/4}(2L'_{\text{nc}} + te^{i\pi/4})$ and $B(s) := \chi(s, L'_{\text{nc}}, te^{i\pi/4}) + \chi(s, L'_{\text{nc}}, 0)$. Thus, for $s_0 \in [0, L_{\text{nc}}]$ and $|s - s_0| < \varepsilon$,

$$|\phi(s, te^{i\pi/4}, \mathbf{z}) - \phi(s_0, te^{i\pi/4}, \mathbf{z})| = \frac{|A| |B(s) - B(s_0)|}{|B(s_0)| |B(s)|} \leq \frac{|A| |B(s) - B(s_0)|}{|B(s_0)| \left| |B(s_0)| - |B(s) - B(s_0)| \right|}. \quad (40)$$

Now $|A| \leq t(2L'_{\text{nc}} + t)$, and, by (30),

$$|B(s_0)| \geq \text{Re} [B(s_0)] \geq L'_{\text{nc}} + \frac{t}{\sqrt{2}} + \sqrt{s_0^2 + L_{\text{nc}}'^2}.$$

Also, $\text{Re} \left[\chi(s, L'_{\text{nc}}, te^{i\pi/4}) \right] > 0$ for $s \in D_\varepsilon$, since $\varepsilon < L'_{\text{nc}}$ so that $\text{Re} \left[s^2 + (L'_{\text{nc}} + te^{i\pi/4})^2 \right] \geq -\text{Im} [s]^2 + L_{\text{nc}}'^2 > 0$. Thus, using (32),

$$\begin{aligned} \left| \chi(s, L'_{\text{nc}}, te^{i\pi/4}) - \chi(s_0, L'_{\text{nc}}, te^{i\pi/4}) \right| &= \frac{|s - s_0| |s + s_0|}{|\chi(s, L'_{\text{nc}}, te^{i\pi/4}) + \chi(s_0, L'_{\text{nc}}, te^{i\pi/4})|} \\ &\leq \frac{\varepsilon(2s_0 + \varepsilon)}{\text{Re} \left[\chi(s_0, L'_{\text{nc}}, te^{i\pi/4}) \right]} \\ &\leq \frac{4\varepsilon(s_0 + L'_{\text{nc}})}{\sqrt{s_0^2 + L_{\text{nc}}'^2}} \leq 4\sqrt{2}\varepsilon. \end{aligned} \quad (41)$$

This implies that $|B(s) - B(s_0)| \leq 8\sqrt{2}\varepsilon$. Inserting these bounds into (40) gives

$$\begin{aligned} |\phi(s, te^{i\pi/4}, \mathbf{z}) - \phi(s_0, te^{i\pi/4}, \mathbf{z})| &\leq \frac{8\sqrt{2}t\varepsilon(2L'_{\text{nc}} + t)}{\left(2L'_{\text{nc}} + t/\sqrt{2}\right) \left(L'_{\text{nc}} + \sqrt{s_0^2 + L_{\text{nc}}'^2} - 8\sqrt{2}\varepsilon\right)} \\ &\leq \frac{L'_{\text{nc}} t}{2\sqrt{2} \sqrt{s_0^2 + L_{\text{nc}}'^2}}, \end{aligned} \quad (42)$$

on using (13). The result (38) follows by combining (39) and (42).

Lemma 47 For $t \geq 0$ and $\mathbf{z} \in \Gamma$, $S_k(s, te^{i\pi/4}, \mathbf{z})$ is analytic as a function of s in D_ε , with ε given by (13). Further, for every $k_0 > 0$,

$$|S_k(s, te^{i\pi/4}, \mathbf{z})| \leq Ck(L'_{\text{nc}} + t)(|\mathbf{z}| + t)^{-1/2}, \quad s \in D_\varepsilon, \quad (43)$$

for $t \geq 0$, $\mathbf{z} \in \Gamma$, and $k \geq k_0$, where $C > 0$ depends only on Ω and k_0 .

Proof Suppose $t \geq 0$ and $\mathbf{z} \in \Gamma$. By (30) and (32) we have, for $s_0 \in [0, L_{\text{nc}}]$,

$$\operatorname{Re} \left[\chi(s_0, L'_{\text{nc}}, te^{i\pi/4}) \right] \geq L'_{\text{nc}}, \quad \operatorname{Re} \left[\chi(z_1, -z_2, te^{i\pi/4}) \right] \geq \frac{|\mathbf{z}| + t}{2}. \quad (44)$$

Combining (44) with (41) and recalling (13) gives

$$\operatorname{Re} \left[\chi(s, L'_{\text{nc}}, te^{i\pi/4}) \right] \geq \frac{7L'_{\text{nc}}}{8}, \quad s \in D_\varepsilon. \quad (45)$$

Therefore, $S_k(s, te^{i\pi/4}, \mathbf{z})$ is analytic in D_ε and, for $k \geq k_0$, applying (27) and (28), we see that (43) holds.

We are now ready to prove Lemma 45.

Proof (Proof of Lemma 45) The analyticity of $K(s, \mathbf{z})$ follows immediately from that of $\phi(s, te^{i\pi/4}, \mathbf{z})$ and $S_k(s, te^{i\pi/4}, \mathbf{z})$, and the fact that the integral (36) converges uniformly for $s \in D_\varepsilon$ in view of the bounds in Lemmas 46 and 47 (see, e.g., [38, §1.88, §4.4]). Further, by Lemmas 46 and 47 we have, for $s \in D_\varepsilon$, that

$$|K(s, \mathbf{z})| \leq CkL'_{\text{nc}}{}^{-5/2}(L'_{\text{nc}} + L_{\text{nc}}) \int_0^\infty \frac{L'_{\text{nc}} + t}{(|\mathbf{z}| + t)^{1/2}} \exp \left[-\frac{kL'_{\text{nc}}t}{2\sqrt{2}\sqrt{L'_{\text{nc}}{}^2 + L_{\text{nc}}{}^2}} \right] dt. \quad (46)$$

The integral in (46) is bounded above by

$$\int_0^\infty \frac{L'_{\text{nc}} + t}{t^{1/2}} \exp \left[-\frac{kL'_{\text{nc}}t}{2\sqrt{2}\sqrt{L'_{\text{nc}}{}^2 + L_{\text{nc}}{}^2}} \right] dt \leq Ck^{-1/2},$$

for $k \geq k_0$, for some $C > 0$ depending only on L'_{nc} , L_{nc} and k_0 . For $k|\mathbf{z}| > 1$ a sharper upper bound is

$$|\mathbf{z}|^{-1/2} \int_0^\infty (L'_{\text{nc}} + t) \exp \left[-\frac{kL'_{\text{nc}}t}{2\sqrt{2}\sqrt{L'_{\text{nc}}{}^2 + L_{\text{nc}}{}^2}} \right] dt \leq Ck^{-1}|\mathbf{z}|^{-1/2}.$$

Combining these two results gives (37).

We now complete the proof of Lemma 43. Applying the Cauchy-Schwarz inequality to (25) gives

$$|W^s(s)| \leq \|K(s, \cdot)\|_{L^2(\Gamma)} \left\| \frac{\partial u}{\partial \mathbf{n}} \right\|_{L^2(\Gamma)}. \quad (47)$$

Recalling (6) and Assumption 22, and that either $\mathcal{A} = \mathcal{A}_{k,\eta}$ (the standard formulation, in which case we assume that $|\eta| \leq Ck$) or $\mathcal{A} = \mathcal{A}_k$ (the star-combined formulation), and recalling the corresponding formulae for f in (6), we see that

$$\left\| \frac{\partial u}{\partial \mathbf{n}} \right\|_{L^2(\Gamma)} \leq \left\| \mathcal{A}^{-1} \right\|_{L^2(\Gamma)} \|f\|_{L^2(\Gamma)} \leq C_1 k^{\beta_1} \|f\|_{L^2(\Gamma)} \leq CC_1 k^{1+\beta_1}, \quad k \geq k_1, \quad (48)$$

where $C > 0$ depends only on Ω and k_1 . It remains to bound $\|K(s, \cdot)\|_{L^2(\Gamma)}$. But, by (37), this just requires a bound on $\|\zeta\|_{L^2(\Gamma)}$. Let Γ^* denote any one of the sides

of Γ . Then it is clear that, if Γ^* is not one of the sides of Γ adjacent to \mathbf{P}' , then $\int_{\Gamma^*} (\zeta(\mathbf{z}))^2 ds \leq Ck^{-1}$, for $k \geq k_0$. On the other hand, if Γ^* has length L^* and is adjacent to \mathbf{P}' , then

$$\int_{\Gamma^*} (\zeta(\mathbf{z}))^2 ds \leq C \int_0^{1/k} ds + Ck^{-1} \int_{1/k}^{L^*} t^{-1} dt \leq Ck^{-1} \log(2+k).$$

Thus $\|\zeta\|_{L^2(\Gamma)} \leq Ck^{-1/2} \log^{1/2}(2+k)$, so that, by (37),

$$\|K(s, \cdot)\|_{L^2(\Gamma)} \leq C \log^{1/2}(2+k), \quad (49)$$

where $C > 0$ depends only on Ω . Finally, combining (47), (48) and (49) proves (24), which completes the proof of Lemma 43.

4.2 Proof of Lemma 42

Suppose first that $\alpha \notin (\pi/2, 3\pi/2)$, in which case both Ψ and Ψ_1 are zero. Then, since $u^i(\mathbf{y}) = e^{iky_2 \cos \alpha}$ for $\mathbf{y} \in \gamma'$, we have

$$-4 \int_{\gamma'} \frac{\partial^2 \Phi_k(\mathbf{x}, \mathbf{y})}{\partial x_2 \partial y_1} u^i(\mathbf{y}) ds(\mathbf{y}) = e^{ikr} W^i(s),$$

where

$$W^i(s) = \int_0^\infty e^{ik\varpi(s, y_2, \alpha)} T_k(s, y_2) dy_2, \quad (50)$$

with

$$\begin{aligned} \varpi(s, y_2, \alpha) &:= \chi(s, L'_{\text{nc}}, y_2) - \chi(s, L'_{\text{nc}}, 0) + y_2 \cos \alpha, \\ T_k(s, y_2) &:= \frac{ik^2 s(L'_{\text{nc}} + y_2)}{[\chi(s, L'_{\text{nc}}, y_2)]^2} H_2^*(k\chi(s, L'_{\text{nc}}, y_2)). \end{aligned}$$

We deform the contour of integration in (50) to $\gamma^* = \{te^{i\pi/4} : t \geq 0\}$, as in (36). Then, arguing as in the proofs of Lemmas 46 and 47, we see that $\varpi(s, te^{i\pi/4}, \alpha)$ and $T_k(s, te^{i\pi/4})$ are analytic as functions of s in D_ε , with ε given by (13). Further, since $\cos \alpha \geq 0$, it follows from the calculations in the proof of Lemma 46 that

$$\text{Im} [\varpi(s, te^{i\pi/4}, \alpha)] \geq \frac{L'_{\text{nc}} t}{2\sqrt{2}\sqrt{L_{\text{nc}}'^2 + L_{\text{nc}}^2}}, \quad s \in D_\varepsilon, t \geq 0, \quad (51)$$

while, from (45) and (28), it follows that, for all $k_0 > 0$,

$$|T_k(s, te^{i\pi/4})| \leq Ck^{3/2}(L'_{\text{nc}} + t),$$

if $s \in D_\varepsilon$, $t \geq 0$, and $k \geq k_0$, where $C > 0$ depends only on Ω and k_0 . Thus

$$|W^i(s)| \leq \int_0^\infty e^{-k\text{Im}[\varpi(s, te^{i\pi/4}, \alpha)]} |T_k(s, te^{i\pi/4})| dt \leq Ck^{1/2}. \quad (52)$$

If $\alpha \in (\pi/2, 3\pi/2)$, however, (51) no longer holds (since $\cos \alpha < 0$). In this case we write $u^i = u^d + (u^i - u^d)$, and note that, by Lemma 35, for $\mathbf{y} \in \gamma'$,

$$u^i(\mathbf{y}) - u^d(\mathbf{y}) = 2e^{iky_2} h\left(\sqrt{2ky_2} \sin(\alpha/2)\right),$$

where $h(w) := e^{-iw^2} \text{Fr}(w)$. The function $h(w)$ is entire, and is uniformly bounded in the sector $\arg[w] \in [-\pi/2, \pi]$ (this follows from the asymptotic behaviour of the complementary error function [1, §7.12(i)], and that $h(w) = \frac{1}{2}e^{-iw^2} \text{erfc}(e^{-i\pi/4}w)$). Hence a similar argument to that leading to (52), but applied to $u^i - u^d$ rather than to u^i , shows that

$$-4 \int_{\gamma'} \frac{\partial^2 \Phi_k(\mathbf{x}, \mathbf{y})}{\partial x_2 \partial y_1} (u^i(\mathbf{y}) - u^d(\mathbf{y})) ds(\mathbf{y}) = e^{ikr} W^i(s), \quad (53)$$

with $W^i(s)$ analytic in D_ε , where it satisfies (52) with $\varpi(s, te^{i\pi/4}, \alpha)$ replaced by $\varpi(s, te^{i\pi/4}, 0)$ and $T_k(s, te^{i\pi/4})$ replaced by $2T_k(s, te^{i\pi/4})h\left(\sqrt{2kt} \sin(\alpha/2) e^{i\pi/8}\right)$; in particular, $|W^i(s)| \leq Ck^{1/2}$ for $k \geq k_0$ and $s \in D_\varepsilon$, where C depends only on k_0 and Ω . The next result deals with the remaining term, $4 \int_{\gamma'} (\partial^2 \Phi_k(\mathbf{x}, \mathbf{y}) / \partial x_2 \partial y_1) u^d(\mathbf{y}) ds(\mathbf{y})$.

Proposition 48

$$u^d(\mathbf{x}) = \Psi_2(\mathbf{x}) - 2 \int_{\gamma'} \frac{\partial \Phi_k(\mathbf{x}, \mathbf{y})}{\partial y_1} u^d(\mathbf{y}) ds(\mathbf{y}), \quad x_1 < 0, \quad (54)$$

where

$$\Psi_2(\mathbf{x}) := \begin{cases} 0, & 0 \leq \alpha \leq \pi, \\ u^i(\mathbf{x}) + (u^i)'(\mathbf{x}) = -2ie^{ikx_2 \cos \alpha} \sin(kx_1 \sin \alpha), & \pi < \alpha < 2\pi. \end{cases}$$

Proof Suppose first that $0 \leq \alpha \leq \pi/2$. Let k temporarily have a positive imaginary part. Then it is straightforward to show that u^d is uniformly bounded in the half-plane $x_1 < 0$, and hence (54) follows from [12, Theorem 3.1] for $\text{Im}[k] > 0$, and for $k > 0$ by taking the limit as $\text{Im}[k] \rightarrow 0$ [12, Theorem 3.2].

For $\pi/2 < \alpha \leq \pi$ this argument fails, since if k has a positive imaginary part, $|u^d(\mathbf{x})|$ grows exponentially as $x_2 \rightarrow \infty$ for any fixed $x_1 < 0$. However, the argument does provide a proof that (54) holds (with $\Psi_2 = 0$) with u^d replaced by $u^d - u^i$, which is uniformly bounded in $x_1 < 0$. Also, the analysis of [12, p. 193] shows that (54) holds (with $\Psi_2 = 0$) with u^d replaced by the plane wave u^i . Adding together these two results proves (54).

The above two paragraphs prove (54) for the case $0 \leq \alpha \leq \pi$ when $\Psi_2 = 0$. For $\pi < \alpha < 2\pi$, the above arguments allow us to prove (54) (with $\Psi_2 = 0$) with u^d replaced by \tilde{u}^d , the solution to the knife edge scattering problem of Figure 4(b) corresponding to the incident direction $2\pi - \alpha \in (0, \pi)$. Since $\tilde{u}^d = u^d - u^i - (u^i)'$, and in particular $\tilde{u}^d = u^d$ on γ' , this implies that

$$u^d(\mathbf{x}) - u^i(\mathbf{x}) - (u^i)'(\mathbf{x}) = -2 \int_{\gamma'} \frac{\partial \Phi_k(\mathbf{x}, \mathbf{y})}{\partial y_1} u^d(\mathbf{y}) ds(\mathbf{y}), \quad x_1 < 0,$$

i.e. that (54) holds for $\pi < \alpha < 2\pi$.

For $\alpha \in (\pi/2, 3\pi/2)$ we have $2\partial\Psi_2/\partial\mathbf{n} = \partial\Psi_1/\partial\mathbf{n}$ on Γ_{nc} , and so it follows from Proposition 48 that, for $\mathbf{x} \in \Gamma_{\text{nc}}$,

$$-4 \int_{\gamma'} \frac{\partial^2 \Phi_k(\mathbf{x}, \mathbf{y})}{\partial x_2 \partial y_1} u^d(\mathbf{y}) \, ds(\mathbf{y}) = 2 \frac{\partial u^d}{\partial \mathbf{n}}(\mathbf{x}) - \frac{\partial \Psi_1}{\partial \mathbf{n}}(\mathbf{x}).$$

Combining this with (53) completes the proof of Lemma 42.

5 hp Approximation Space and Approximation Results

We now design an hp approximation space for the numerical solution of (6), based on the regularity results provided by Theorems 32 and 36. Rather than approximating $\partial u/\partial\mathbf{n}$ itself, we will approximate

$$\varphi(\mathbf{x}) := \frac{1}{k} \left(\frac{\partial u}{\partial \mathbf{n}}(\mathbf{x}) - \Psi(\mathbf{x}) \right), \quad \mathbf{x} \in \Gamma, \quad (55)$$

which represents the difference between $\partial u/\partial\mathbf{n}$ and the known leading order high frequency behaviour Ψ (as discussed in Remarks 34 and 37), scaled by $1/k$ so that φ is nondimensional. This leading order behaviour is that defined in Theorems 32 and 36. Thus, on a convex side, $\Psi := 2\partial u^i/\partial\mathbf{n}$ if the side is illuminated and $\Psi := 0$ otherwise. On a nonconvex side, $\Psi := 2u^i(\mathbf{P}')\partial u^d/\partial\mathbf{n}$ if $\pi/2 \leq \alpha \leq 3\pi/2$, and $\Psi := 0$ otherwise; here u^d is defined as in Lemma 35 in terms of the local variables r, θ, α of Figure 4(a) (as remarked previously, any nonconvex side can be transformed to the configuration in Figure 4(a) by a suitable rotation and reflection of Ω). The factor $u^i(\mathbf{P}')$ is a phase shift arising because the origin of the global coordinates \mathbf{x} may not be located at the point \mathbf{P}' , as was assumed in Theorem 36.

Instead of approximating φ directly by conventional piecewise polynomials, on each side of the polygon we use the appropriate representation (9) or (12), with the non-oscillatory coefficients v^\pm and v replaced by piecewise polynomial approximations supported on overlapping meshes, graded towards corner singularities (where these are present). Before detailing the approximation space, we introduce some notation.

Definition 51 *Given $-\infty < a < b < \infty$ and an integer $p \geq 0$, let $\mathcal{P}_p(a, b)$ denote the space of polynomials on (a, b) of degree $\leq p$. Given $A > 0$ and an integer $n \geq 1$ we denote by $\mathcal{G}_n(0, A) = \{x_0, x_1, \dots, x_n\}$ the geometric mesh on $[0, A]$ with n layers, whose meshpoints x_i are defined by*

$$x_0 := 0, \quad x_i := \sigma^{n-i} A, \quad i = 1, 2, \dots, n,$$

where $0 < \sigma < 1$ is a fixed grading parameter. We denote by $\mathcal{P}_{p,n}(0, A)$ the space of piecewise polynomials on $\mathcal{G}_n(0, A)$ with degree $\leq p$, i.e.

$$\mathcal{P}_{p,n}(0, A) := \{ \rho : [0, A] \rightarrow \mathbb{C} : \rho|_{(x_{i-1}, x_i)} \in \mathcal{P}_p(x_{i-1}, x_i), i = 1, \dots, n \}.$$

A smaller value of σ represents a more severe grading. While the value $\sigma = (\sqrt{2} - 1)^2 \approx 0.17$ is in some sense optimal, e.g., [35, p.96], it is common practice to slightly “overrefine” by taking $\sigma = 0.15$; we use this value in the computations in §7.

We will approximate using the graded mesh in the above definition on each side of the polygon, using throughout the same polynomial degree (p) and the same number of layers (n) in each graded mesh. We will assume that, for some fixed constant $c > 0$, it holds that

$$n \geq cp. \quad (56)$$

On a convex side Γ_c , we recall from (9) that

$$\varphi(\mathbf{x}(s)) = \frac{1}{k} \left(v^+(s)e^{iks} + v^-(L_c - s)e^{-iks} \right), \quad s \in [0, L_c],$$

where the coefficients $v^+(s)$ and $v^-(L_c - s)$ are singular at $s = 0$ and $s = L_c$, respectively. To approximate φ on Γ_c we approximate $v^+(s) \approx \rho^+(s)$ and $v^-(L_c - s) \approx \rho^-(L_c - s)$, for some $\rho_{\pm} \in \mathcal{P}_{p,n}(0, L_c)$.

On a nonconvex side Γ_{nc} , we recall from (12) that

$$\varphi(\mathbf{x}(s)) = \frac{1}{k} \left(v^+(L_{nc} + s)e^{iks} + v^-(L_{nc} - s)e^{-iks} + v(s)e^{ikr} \right), \quad s \in [0, L_{nc}].$$

The coefficient $v^-(L_{nc} - s)$ is singular at $s = L_{nc}$, but the coefficients $v^+(L_{nc} + s)$ and $v(s)$ are both analytic in a neighbourhood of $[0, L_{nc}]$ and can be approximated by single polynomials supported on the whole side. To approximate φ on Γ_{nc} we therefore approximate $v^-(L_{nc} - s) \approx \rho^-(L_{nc} - s)$ for some $\rho^- \in \mathcal{P}_{p,n}(0, L_{nc})$, and approximate $v^+(L_{nc} + s) \approx \rho^+(s)$ and $v(s) \approx \rho(s)$ for some $\rho^+, \rho \in \mathcal{P}_p(0, L_{nc})$. An illustration of the resulting meshes is given in Figure 5.

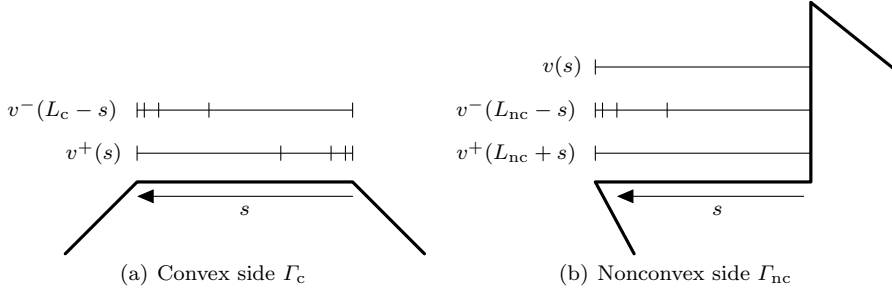


Fig. 5 Illustration of the overlapping meshes used to approximate the solution components indicated.

The above construction amounts to constraining the approximation to φ to lie in a particular finite-dimensional approximation space $V_{N,k} \subset L^2(\Gamma)$, of dimension N (the total number of degrees of freedom), given by

$$N = (p+1)(2nn_c + (n+2)n_{nc}), \quad (57)$$

where n_c and n_{nc} denote the number of convex and nonconvex sides, respectively.

For $a < b$ and $r > b - a$, let

$$\mathcal{E}_{a,b,r} := \{w \in \mathbb{C} : |w - a| + |w - b| < r\}, \quad (58)$$

the interior of an ellipse with foci $\{a, b\}$. Our best approximation estimates are based on the following standard result, which follows from [37, Theorem 2.1.1].

Lemma 52 *If the function g is analytic and bounded in $\mathcal{E}_{a,b,r}$, for some $a, b, r \in \mathbb{R}$ with $a < b$ and $r > b - a$, then*

$$\inf_{v' \in \mathcal{P}_p(a,b)} \|g - v'\|_{L^\infty(a,b)} \leq \frac{2}{\rho - 1} \rho^{-p} \|g\|_{L^\infty(\mathcal{E}_{a,b,r})},$$

where $\rho = (r + \sqrt{r^2 - (b - a)^2}) / (b - a) > 1$.

Lemma 52 implies the following best approximation results for the two non-singular terms in the representation on a nonconvex side.

Theorem 53 *Suppose that Assumption 22 holds. Then, for every $k_0 > 0$, for the approximation of $v^+(L_{\text{nc}} + s)$ on a nonconvex side Γ_{nc} we have*

$$\inf_{v' \in \mathcal{P}_p(0, L_{\text{nc}})} \|v^+(L_{\text{nc}} + \cdot) - v'\|_{L^2(0, L_{\text{nc}})} \leq CM(u)k^{1/2}e^{-p\tau}, \quad k \geq k_0,$$

where $\tau = \log(2 + \sqrt{3})$ and $C > 0$ depends only on Ω and k_0 .

Proof By Theorem 36, $v_+(s)$ is analytic in $\text{Re}[s] > 0$ where it satisfies the bound (10). Thus $g(s) := v^+(L_{\text{nc}} + s)$ is analytic in $\text{Re}[s] > -L_{\text{nc}}$, in particular analytic and bounded in $\text{Re}[s] > -L_{\text{nc}}/2$, which contains the ellipse $\mathcal{E}_{0, L_{\text{nc}}, r}$ with $r = 2L_{\text{nc}}$. Thus combining Lemma 52 with (10) gives

$$\inf_{v' \in \mathcal{P}_p(0, L_{\text{nc}})} \|v^+(L_{\text{nc}} + \cdot) - v'\|_{L^\infty(0, L_{\text{nc}})} \leq CM(u)k^{1/2}\rho^{-p},$$

with $\rho = 2 + \sqrt{3}$, from which the result follows.

Theorem 54 *Suppose that Assumption 22 holds. Then, where k_1, β_1 , and C_1 are the constants in that assumption, for the approximation of $v(s)$ on a nonconvex side Γ_{nc} we have*

$$\inf_{v' \in \mathcal{P}_p(0, L_{\text{nc}})} \|v - v'\|_{L^2(0, L_{\text{nc}})} \leq CC_1 k^{1+\beta_1} \log^{1/2}(2+k)e^{-p\tau}, \quad k \geq k_1,$$

where $\tau = \log(\sqrt{1 + (2\varepsilon/L_{\text{nc}})^2} + 2\varepsilon/L_{\text{nc}})$, ε is given by (13), and $C > 0$ depends only on Ω and k_1 .

Proof By Theorem 36 $v(s)$ is analytic and bounded in $D_\varepsilon \supset \mathcal{E}_{0, L_{\text{nc}}, \varepsilon}$. The result follows by combining Lemma 52 with (14).

The remaining terms all have singularities associated with corner singularities requiring geometric mesh refinement. Let

$$\delta_* := 1 - \pi/\omega_{\min} \in (0, 1/2), \quad (59)$$

where ω_{\min} denotes the smallest of the exterior angles of the polygon that are larger than π . Arguing as in [28, §5] one can use Lemma 52 to prove:

Theorem 55 (cf. [28, Theorem 5.4]) *Suppose that Assumption 22 and (56) hold. Then, for every $k_0 > 0$, for the approximation of $v^+(s)$ and $v^-(L_c - s)$ on a convex side Γ_c we have*

$$\inf_{v' \in \mathcal{P}_{p,n}(0, L_c)} \|v^\pm - v'\|_{L^2(0, L_c)} \leq CM(u)k^{1-\delta_*} e^{-p\tau}, \quad k \geq k_0,$$

where $\tau > 0$ depends only on σ , the corner angles at the ends of Γ_c , and c (the constant in (56)), and $C > 0$ only on Ω and k_0 . The same estimate holds for the approximation of $v^-(L_{nc} - s)$ on a nonconvex side, except that L_c is replaced by L_{nc} in the above formula, and τ depends now on σ , c , and the exterior angle ω in Figure 4(a).

We now combine these results into a single estimate for the best approximation error associated with the approximation of $\varphi \in L^2(\Gamma)$ by an element of $V_{N,k}$. From (9), (12), (55), Theorems 53, 54, and 55, and the definition of the approximation space $V_{N,k}$, the following result follows:

Theorem 56 *Suppose that Assumption 22 and (56) hold. Then, where k_1 , β_1 , C_1 , and c are the constants in those assumptions, we have*

$$\inf_{v' \in V_{N,k}} \|\varphi - v'\|_{L^2(\Gamma)} \leq C(M(u)k^{-\delta_*} + k^{\beta_1} \log^{1/2}(2+k)) e^{-p\tau}, \quad k \geq k_1, \quad (60)$$

where $C > 0$ depends only on C_1 , Ω and k_1 , and $\tau > 0$ depends only on c , σ , and Ω .

6 Galerkin Method

Having designed an approximation space $V_{N,k}$ which can efficiently approximate φ , we will select an element of $V_{N,k}$ by applying the Galerkin method to the integral equation (6), rewritten with φ defined by (55) as the unknown. That is, we seek $\varphi_N \in V_{N,k} \subset L^2(\Gamma)$ such that

$$\langle \mathcal{A}\varphi_N, v \rangle_{L^2(\Gamma)} = \frac{1}{k} \langle f - \mathcal{A}\Psi, v \rangle_{L^2(\Gamma)}, \quad \text{for all } v \in V_{N,k}. \quad (61)$$

If Assumption 23 holds, which is proved for the case $\mathcal{A} = \mathcal{A}_k$ when Ω is starlike, and we conjecture holds for all Ω in our class \mathcal{C} for the choice $\mathcal{A} = \mathcal{A}_{k,k}$ (see the discussion at the end of §2), then existence and uniqueness of the Galerkin solution φ_N is guaranteed by the Lax-Milgram lemma. Moreover, by Céa's lemma (e.g., [14, Lemma 6.9]) we have the quasi-optimality estimate

$$\|\varphi - \varphi_N\|_{L^2(\Gamma)} \leq \frac{C_0 k^{1/2}}{C_2} \inf_{v' \in V_{N,k}} \|\varphi - v'\|_{L^2(\Gamma)}, \quad k \geq k_2, \quad (62)$$

where C_2 and k_2 are the constants from Assumption 23, and C_0 is the constant from Lemma 21 in the case that $k_0 = k_2$. Combined with Theorem 56, this gives:

Theorem 61 *Suppose that Assumption 23 and (56) hold. Then, where k_2 , β_2 , C_2 , and c are the constants in those assumptions, we have*

$$\|\varphi - \varphi_N\|_{L^2(\Gamma)} \leq Ck^{1/2}(M(u)k^{-\delta_*} + k^{\beta_2} \log^{1/2}(2+k)) e^{-p\tau}, \quad k \geq k_2, \quad (63)$$

where $C > 0$ depends only on C_2 , Ω and k_2 , and $\tau > 0$ depends only on c , σ , and Ω .

An approximation u_N to the solution u of the BVP can be found by inserting the approximation $\partial u/\partial \mathbf{n} \approx \Psi + k\varphi_N$ into the formula (5), i.e.

$$u_N(\mathbf{x}) := u^i(\mathbf{x}) - \int_{\Gamma} \Phi_k(\mathbf{x}, \mathbf{y}) (\Psi(\mathbf{y}) + k\varphi_N(\mathbf{y})) \, ds(\mathbf{y}), \quad \mathbf{x} \in D.$$

Arguing exactly as in the proof of [28, Theorem 6.3], noting that $M(u) = \|u\|_{L^\infty(D)} \geq 1$ (since $|u(\mathbf{x})| \sim |u^i(\mathbf{x})| = 1$ as $|\mathbf{x}| \rightarrow \infty$), we deduce:

Theorem 62 *Under the assumptions of Theorem 61 we have*

$$\frac{\|u - u_N\|_{L^\infty(D)}}{\|u\|_{L^\infty(D)}} \leq Ck \log^{1/2}(2+k)(k^{-\delta_*} + k^{\beta_2} \log^{1/2}(2+k)) e^{-p\tau}, \quad k \geq k_2, \quad (64)$$

where $C > 0$ depends only on C_2 , Ω and k_2 , and $\tau > 0$ depends only on c , σ , and Ω .

An object of interest in applications is the *far field pattern* of the scattered field. An asymptotic expansion of the representation (5) reveals that (cf. [20])

$$u^s(\mathbf{x}) \sim \frac{e^{i\pi/4}}{2\sqrt{2\pi}} \frac{e^{ikr}}{\sqrt{kr}} F(\hat{\mathbf{x}}), \quad \text{as } r := |\mathbf{x}| \rightarrow \infty, \quad (65)$$

where $\hat{\mathbf{x}} := \mathbf{x}/|\mathbf{x}| \in \mathbb{S}^1$, the unit circle, and

$$F(\hat{\mathbf{x}}) := - \int_{\Gamma} e^{-ik\hat{\mathbf{x}} \cdot \mathbf{y}} \frac{\partial u}{\partial \mathbf{n}}(\mathbf{y}) \, ds(\mathbf{y}), \quad \hat{\mathbf{x}} \in \mathbb{S}^1. \quad (66)$$

An approximation F_N to the far field pattern F can be found by inserting the approximation $\partial u/\partial \mathbf{n} \approx \Psi + k\varphi_N$ into the formula (66), i.e.

$$F_N(\hat{\mathbf{x}}) := - \int_{\Gamma} e^{-ik\hat{\mathbf{x}} \cdot \mathbf{y}} (\Psi(\mathbf{y}) + k\varphi_N(\mathbf{y})) \, ds(\mathbf{y}), \quad \hat{\mathbf{x}} \in \mathbb{S}^1. \quad (67)$$

The proof of the following estimate follows precisely that of [28, Theorem 6.4].

Theorem 63 *Under the assumptions of Theorem 61 we have*

$$\|F - F_N\|_{L^\infty(\mathbb{S}^1)} \leq Ck^{3/2}(M(u)k^{-\delta_*} + k^{\beta_2} \log^{1/2}(2+k)) e^{-p\tau}, \quad k \geq k_2, \quad (68)$$

where $C > 0$ depends only on C_2 , Ω and k_2 , and $\tau > 0$ depends only on c , σ , and Ω .

The above results hold for all polygons Ω in the class \mathcal{C} defined in Definition 31, provided that Assumption 23 holds. If, in addition, Ω is star-like, it has been shown in [28, Theorem 4.3] (see Remark 33) that

$$M(u) \leq Ck^{1/2} \log^{1/2}(2+k), \quad k \geq k_2, \quad (69)$$

where C depends only on k_2 and Ω . Further, as remarked above, if $\mathcal{A} = \mathcal{A}_k$, then it is shown in [36] that Assumption 23 holds for every $k_2 > 0$, moreover with $\beta_2 = 0$. Thus the above results have the following corollary which requires no coercivity assumption.

Corollary 64 *Suppose that Ω is a star-like member of the class \mathcal{C} . Suppose also that we choose $\mathcal{A} = \mathcal{A}_k$, the star-combined potential operator defined in (8), and that we choose n so that (56) holds. Then, for any $k_2 > 0$, for $k \geq k_2$ we have*

$$\|\varphi - \varphi_N\|_{L^2(\Gamma)} \leq Ck^{1-\delta_*} \log^{1/2}(2+k) e^{-p\tau}, \quad (70)$$

$$\frac{\|u - u_N\|_{L^\infty(D)}}{\|u\|_{L^\infty(D)}} \leq Ck \log(2+k) e^{-p\tau}, \quad (71)$$

$$\|F - F_N\|_{L^\infty(\mathbb{S}^1)} \leq Ck^{2-\delta_*} \log^{1/2}(2+k) e^{-p\tau}, \quad (72)$$

where $C > 0$ depends only on Ω and k_2 , and $\tau > 0$ depends only on c , σ , and Ω .

Remark 65 *As remarked above and at the end of §2, it is reasonable, based on the numerical evidence in [6], to conjecture that Assumption 23 holds for every $k_2 > 0$ also for the choice $\mathcal{A} = \mathcal{A}_{k,k}$, moreover with $\beta_2 = 0$. Thus we conjecture that the bounds in the above corollary hold also for $\mathcal{A} = \mathcal{A}_{k,k}$.*

Remark 66 *The algebraically k -dependent prefactors in the error estimates derived in this section can be absorbed into the exponentially decaying factors by allowing p to grow modestly with increasing k . We illustrate this in the case of (71). If we assume that*

$$p \geq \frac{\log(k \log(2+k))}{c_0},$$

for some $0 < c_0 < \tau$, then (71) can be replaced by

$$\frac{\|u - u_N\|_{L^\infty(D)}}{\|u\|_{L^\infty(D)}} \leq Ce^{-p\kappa}, \quad k \geq k_2, \quad (73)$$

where $\kappa = \tau - c_0$, and both C and κ are independent of k . Since the number of degrees of freedom, N , is given by (57), and it is sufficient to increase n in proportion to p for (73) to hold, it follows from (73) that, to maintain a fixed accuracy, we need only increase N in proportion to $(\log(k \log k))^2$ as $k \rightarrow \infty$.

7 Numerical Results

We present numerical computations of the Galerkin approximation φ_N defined by (61), using the standard combined-potential formulation, $\mathcal{A} = \mathcal{A}_{k,k}$, given by (7), for a particular starlike scatterer in the class \mathcal{C} . In contrast to the choice $\mathcal{A} = \mathcal{A}_k$, the star-combined operator given by (8), for which Corollary 64 holds, we do not have a complete theory for $\mathcal{A} = \mathcal{A}_{k,k}$ in the sense that, while Theorems 61–63 apply, Assumption 23 has not been shown to hold for obstacles in the class \mathcal{C} for $\mathcal{A} = \mathcal{A}_{k,k}$. One point of the computations in this section is to provide evidence for the conjecture in Remark 65 that (70)–(72) hold also for $\mathcal{A} = \mathcal{A}_{k,k}$.

In all of our experiments we take $n = 2(p+1)$. From (57), the total number of degrees of freedom is thus given by $N = 12p^2 + 28p + 16$. The scatterer we consider is shown in Figure 2(b). Its nonconvex sides have length 2π and its convex sides length 4π , so that the total length of the boundary is 12π , which is $6k$ wavelengths since the wavelength $\lambda = 2\pi/k$. We consider two different incident directions α , measured anticlockwise from the downwards vertical:

1. $\alpha = 5\pi/4$, as shown in Figure 1(a); in this case, multiply-reflected rays are present in the asymptotic solution.
2. $\alpha = 5\pi/3$, as shown in Figure 1(b); in this case, one of the nonconvex sides is partially illuminated.

The scatterers, the incident directions, the corresponding total fields for $k = 10$, and a circle of radius 3π on which we compute the total field for the purpose of calculating errors (see Figure 8 below) are plotted in Figure 1. We will demonstrate exponential decay of $\|\varphi - \varphi_N\|_{L^2(\Gamma)}$ as p increases, for fixed k , as predicted by (63). More significantly, we will also see that, as k increases with p fixed, $\|\varphi - \varphi_N\|_{L^2(\Gamma)}$ actually decreases, so that the method is more accurate for the examples considered than suggested by the bound (70), maintaining accuracy as $k \rightarrow \infty$ with a fixed number of degrees of freedom. Similarly, we will see that the relative error, $\|\varphi - \varphi_N\|_{L^2(\Gamma)} / \|\varphi\|_{L^2(\Gamma)}$, grows only very slowly as k increases with N fixed. We will also compute the solution in the domain and the far field pattern, making comparison with the error estimates (71) and (72).

Since N depends only on p , and the values of p are more intuitively meaningful, we introduce the additional notation $\psi_p(s) := \varphi_N(s)$. We begin in Figure 6 by plotting $|\psi_p(s)|$ (sampled at 100,000 evenly spaced points on the boundary) for $\alpha = 5\pi/3$ and $k = 10$ and 160. The corner between the two nonconvex sides is at

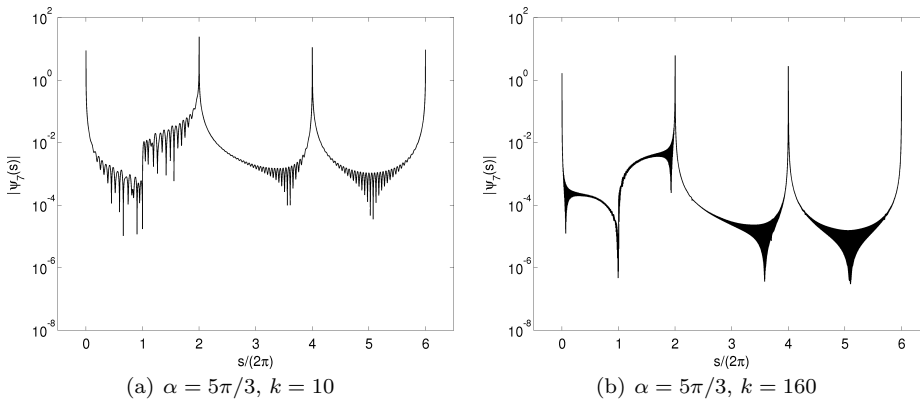


Fig. 6 Boundary solution for $\alpha = 5\pi/3$, with $k = 10$ and $k = 160$.

$s/(2\pi) = 1$; the corners between convex and nonconvex sides are at $s/(2\pi) = 2$ and $s/(2\pi) = 0$ (equivalently, by periodicity, $s/(2\pi) = 6$), and the corner between the two convex sides is at $s/(2\pi) = 4$. There is a singularity in the solution φ at all corners except the one between the nonconvex sides, where $\varphi = 0$. These singularities are evident in Figure 6 as is the increased oscillation for larger k . (The apparent shaded region is an artefact of very high oscillation.)

In Figure 7 we plot the relative L^2 and L^1 errors against p , for the two angles of incidence, for three values of k . We take the “exact” reference solutions to be those computed with $p = 7$, as plotted in Figure 6 for the case $\alpha = 5\pi/3$. The L^2 and L^1 norms are computed by high-order composite Gaussian quadrature on a

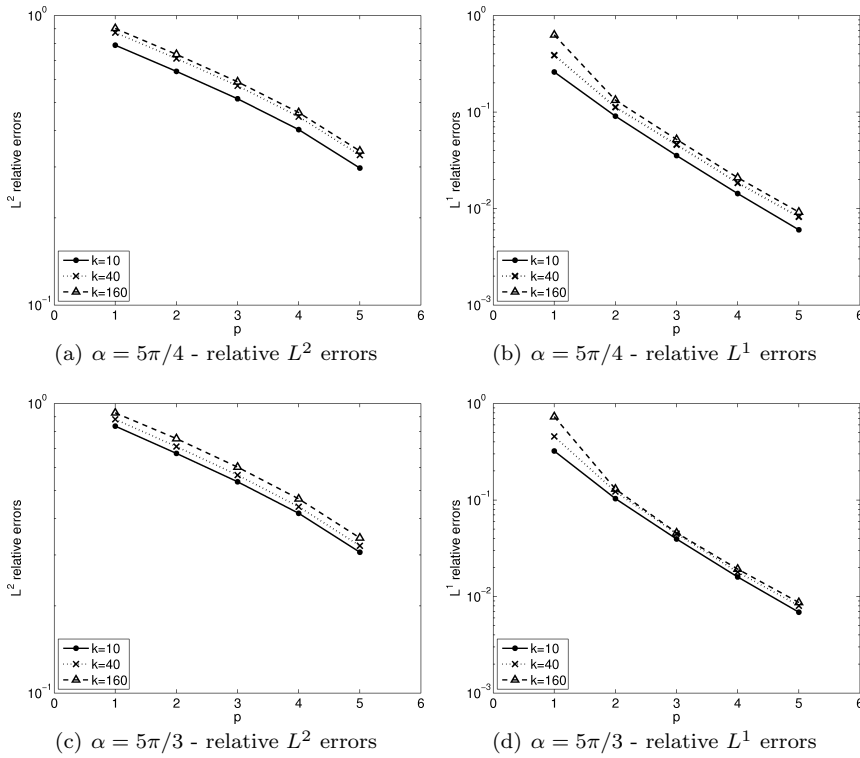


Fig. 7 Relative L^2 and L^1 errors in boundary solution.

mesh graded towards the corner singularities; experimental evidence suggests that these calculations are accurate to at least two significant figures.

Figure 7 shows the exponential decay as p increases that is predicted for the L^2 error by (63). A key question is how the accuracy depends on k ; we see that in all four plots in Figure 7 the relative errors increase only very mildly as k increases. To investigate this further, in Table 1 we show results for the two angles of incidence for $p = 4$ (and hence $N = 320$), for a range of k . We tabulate L^2 errors, relative L^2 and L^1 errors, and also $N/(L/\lambda)$, the average number of degrees of freedom per wavelength. As k increases, the relative errors increase very slowly, the absolute L^2 error actually decreases, while the average number of degrees of freedom per wavelength decreases in proportion to k^{-1} . We also tabulate $\log_2(\text{error}(2k)/\text{error}(k))$, where $\text{error}(k)$ refers to the absolute L^2 error for a particular value of k . This is an estimate of the order of convergence, μ , on a hypothesis that $\text{error}(k) \sim k^\mu$ as $k \rightarrow \infty$. Since, for this scatterer, $\delta_* \approx 0.4350$, a value $\mu \approx 0.5650$ is the largest consistent with the bound (70). In fact, we see values in the range $(-0.91, -0.19)$, suggestive that the bound (70) overestimates the error growth as k increases. In part this overestimate may be due to using the bound (69) to get (70); as noted in Remark 33 we conjecture that in fact $M(u) = \mathcal{O}(1)$ as $k \rightarrow \infty$.

We now return to Figure 7 where we see that the L^2 errors, while decreasing exponentially as p increases, are large in absolute value. Errors of a similar mag-

Table 1 L^2 and L^1 errors for each example, fixed $p = 4$ (and hence $N = 320$), various k , with $N/(L/\lambda)$ the average number of degrees of freedom per wavelength along the boundary.

α	k	$\frac{N}{L/\lambda}$	$\ \psi_7 - \psi_4\ _{L^2(\Gamma)}$	μ	$\frac{\ \psi_7 - \psi_4\ _{L^2(\Gamma)}}{\ \psi_7\ _{L^2(\Gamma)}}$	$\frac{\ \psi_7 - \psi_4\ _{L^1(\Gamma)}}{\ \psi_7\ _{L^1(\Gamma)}}$
$5\pi/4$	5	10.67	8.37×10^{-1}	-0.35	3.90×10^{-1}	1.03×10^{-2}
	10	5.33	6.55×10^{-1}	-0.19	4.04×10^{-1}	1.43×10^{-2}
	20	2.67	5.72×10^{-1}	-0.29	4.24×10^{-1}	1.69×10^{-2}
	40	1.33	4.68×10^{-1}	-0.91	4.47×10^{-1}	1.85×10^{-2}
	80	0.67	2.48×10^{-1}	-0.20	4.39×10^{-1}	1.91×10^{-2}
	160	0.33	2.16×10^{-1}		4.62×10^{-1}	2.09×10^{-2}
$5\pi/3$	5	10.67	8.64×10^{-1}	-0.46	4.05×10^{-1}	1.17×10^{-2}
	10	5.33	6.30×10^{-1}	-0.54	4.18×10^{-1}	1.60×10^{-2}
	20	2.67	4.32×10^{-1}	-0.46	4.27×10^{-1}	1.80×10^{-2}
	40	1.33	3.15×10^{-1}	-0.46	4.40×10^{-1}	1.80×10^{-2}
	80	0.67	2.30×10^{-1}	-0.45	4.54×10^{-1}	1.88×10^{-2}
	160	0.33	1.69×10^{-1}		4.69×10^{-1}	1.92×10^{-2}

nitide are seen in the corresponding convex case [28]. There it is noted that the L^2 errors blow up as the largest exterior angle, ω_{\max} , approaches 2π , this because $\|\varphi\|_{L^2(\Gamma)}$ itself blows up in the same limit (this can be seen from the bound (10) which is sharp in the limit $s \rightarrow 0$). Thus large L^2 errors are inevitable for ω_{\max} close to 2π . A “solution” is to measure errors in a more appropriate norm: in particular this blow up is not seen in the L^1 norm and, indeed, the relative L^1 errors in Figure 7 are 20–40 times smaller.

We now turn our attention to the approximation of $u(\mathbf{x})$, $\mathbf{x} \in D$, and of the far field pattern F (often the quantities of real interest in scattering problems). As is common for linear functionals of the solution on the boundary, the errors in $u(\mathbf{x})$ and $F(\hat{\mathbf{x}})$ are, in general, much smaller than the relative errors in φ . To investigate the accuracy of $u_N(\mathbf{x})$, we compute the error in this solution on a circle of radius 3π surrounding the scatterer, as illustrated in Figure 1. To allow easy comparison between different discretizations, noting again that for each example N depends only on p , we denote the solution on this circle (with a slight abuse of notation) by $u_p(t) := u_N(\mathbf{x}(t))$, $t \in [0, 2\pi]$, where $t = 0$ corresponds to the direction from which u^i is incident, and $\mathbf{x}(t)$ is a point at angular distance t around the circle.

In Figure 8 we plot for each example the relative maximum error on the circle,

$$\frac{\max_{t \in [0, 2\pi]} |u_7(t) - u_p(t)|}{\max_{t \in [0, 2\pi]} |u_7(t)|},$$

computed over 30,000 evenly spaced points in $[0, 2\pi]$, for $k = 10, 40$, and 160. The exponential decay as p increases predicted by Theorem 62 is clear. Moreover, for fixed $p \geq 2$, the relative maximum error decreases as k increases; this is better than the mild growth with k of the bound (71). These relative errors are much smaller than those on the boundary in Figure 7.

Finally, we compute our approximation (67) to the far field pattern. Again, with a slight abuse of notation, we define $F_p(t) := F_N(\hat{\mathbf{x}}(t))$, $t \in [0, 2\pi]$, where $t = 0$ corresponds to the direction from which u^i is incident and $\hat{\mathbf{x}}(t)$ is a point at angular distance t around the unit circle. Plots of $|F_7(t)|$ (the magnitude of the far field pattern computed with our finest discretization), for $k = 10$ and 160 and the two incident directions, are shown in Figure 9. In Figure 10 we plot

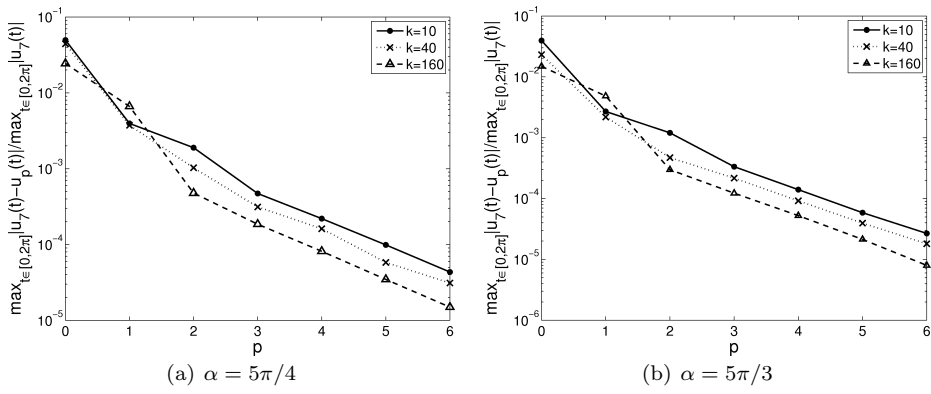


Fig. 8 Relative maximum errors on the circle of Figure 1.

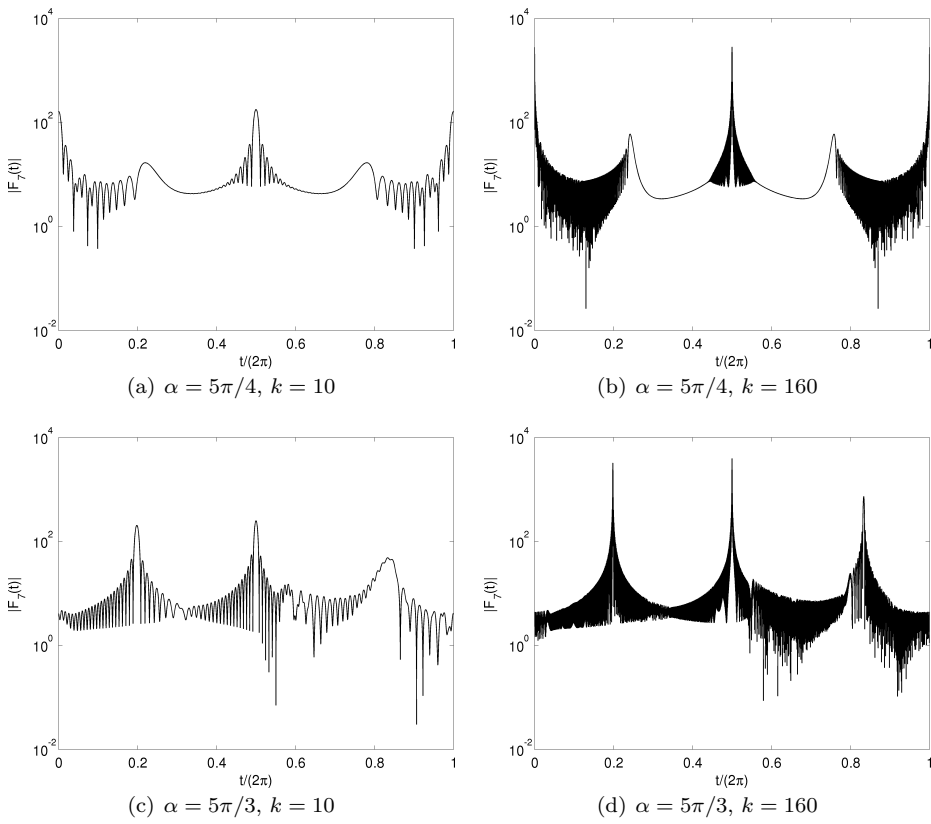


Fig. 9 Far field patterns, $|F_7(t)| \approx |F(t)|$, $k = 10$ and $k = 160$.

approximations to $\|F_7 - F_p\|_{L^\infty(\mathbb{S}^1)}$ for $k = 10, 40,$ and 160 , for the two incident directions. To approximate the L^∞ norm, we compute F_7 and F_p at 30,000 evenly

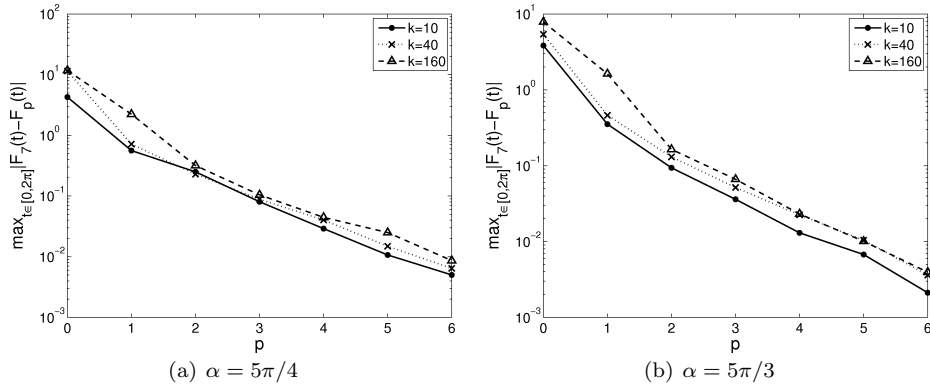


Fig. 10 Absolute maximum errors $\|F_7 - F_p\|_{L^\infty(0, 2\pi)}$ in the far field pattern.

spaced points on the unit circle. The exponential decay as p increases predicted by Theorem 63 is clearly seen. For fixed p , the error does not grow significantly as k increases, indicating that the mild k -dependence of the bound (72) may not be optimal. The errors are comparable in magnitude for each incidence angle, suggesting that our algorithm copes equally well with cases of multiple reflection and partial illumination.

In summary, our numerical examples demonstrate that the predicted exponential convergence of our hp scheme is achieved in practice. Moreover, for a fixed number of degrees of freedom, the accuracy of our numerical solution appears to deteriorate only very slowly (or not at all) as the wavenumber k increases. The p - and k -dependence of our results appears to mimic closely that of the comparable results for the convex polygon in [28]. The k -explicit error bounds in Corollary 64 predict at worst a mild growth in errors as k increases, which can be controlled by a logarithmic growth in the degrees of freedom N , as discussed in Remark 66. The numerical results support the conjecture that this mild growth is pessimistic; the estimates in Corollary 64 are not quite sharp in their k -dependence. We suspect that this is due to lack of sharpness in the dependence on k of the estimate (69) for $M(u)$, of our best approximation estimate (60), and of the quasi-optimality estimate (62).

References

1. Digital Library of Mathematical Functions. National Institute of Standards and Technology, from <http://dlmf.nist.gov/>, release date: 2010-05-07
2. Abboud, T., Nédélec, J.C., Zhou, B.: Méthode des équations intégrales pour les hautes fréquences. *C. R. Math. Acad. Sci. Paris* **318**(2), 165–170 (1994)
3. Anand, A., Boubendir, Y., Ecevit, F., Reitich, F.: Analysis of multiple scattering iterations for high-frequency scattering problems. II: The three-dimensional scalar case. *Numer. Math.* **114**(3), 373–427 (2010)

4. Antoine, X., Chniti, C., Ramdani, K.: On the numerical approximation of high-frequency acoustic multiple scattering problems by circular cylinders. *J. Comput. Phys.* **227**, 1754–1771 (2008)
5. Betcke, T., Chandler-Wilde, S.N., Graham, I.G., Langdon, S., Lindner, M.: Condition number estimates for combined potential boundary integral operators in acoustics and their boundary element discretisation. *Numer. Methods PDEs* **27**(1), 31–69 (2011)
6. Betcke, T., Spence, E.A.: Numerical estimation of coercivity constants for boundary integral operators in acoustic scattering. *SIAM J. Numer. Anal.* **49**(4), 1572–1601 (2011)
7. Borovikov, V.A., Kinber, B.Y.: Geometrical Theory of Diffraction, *IEE Electromagnetic Waves Series*, vol. 37. Institution of Electrical Engineers (IEE), London (1994)
8. Bowman, J.J., Senior, T.B.A., Uslenghi, P.L.E.: Electromagnetic and acoustic scattering by simple shapes. New York, Hemisphere Publishing Corp. (1987)
9. Bruno, O.P.: Fast, high-order, high-frequency integral methods for computational acoustics and electromagnetics. In: Topics in Computational Wave Propagation, *Lect. Notes Comput. Sci. Eng.*, vol. 31, pp. 43–82. Springer (2003)
10. Bruno, O.P., Geuzaine, C.A., Monro, J.A., Reitich, F.: Prescribed error tolerances within fixed computational times for scattering problems of arbitrarily high frequency: the convex case. *Philos. Trans. R. Soc. Lond. Ser. A* **362**(1816), 629–645 (2004)
11. Bruno, O.P., Reitich, F.: High order methods for high-frequency scattering applications. In: H. Ammari (ed.) Modeling and Computations in Electromagnetics, *Lect. Notes Comput. Sci. Eng.*, vol. 59, pp. 129–164. Springer (2007)
12. Chandler-Wilde, S.N.: Boundary value problems for the Helmholtz equation in a half-plane. In: Proc. Third Int. Conf. on Mathematical and Numerical Aspects of Wave Propagation, pp. 188–197. SIAM (1995)
13. Chandler-Wilde, S.N., Graham, I.G., Langdon, S., Lindner, M.: Condition number estimates for combined potential boundary integral operators in acoustic scattering. *J. Integral Equations Appl.* **21**(2), 229–279 (2009)
14. Chandler-Wilde, S.N., Graham, I.G., Langdon, S., Spence, E.A.: Numerical-asymptotic boundary integral methods in high-frequency acoustic scattering. *Acta Numer.* **21**, 89–305 (2012)
15. Chandler-Wilde, S.N., Hewett, D.P., Langdon, S., Twigger, A.: A high frequency BEM for scattering by non-convex obstacles. In: Proc. 10th Int. Conf. on Mathematical and Numerical Aspects of Waves, Vancouver, Canada, pp. 307–310 (2011)
16. Chandler-Wilde, S.N., Langdon, S.: A Galerkin boundary element method for high frequency scattering by convex polygons. *SIAM J. Numer. Anal.* **45**(2), 610–640 (2007)
17. Chandler-Wilde, S.N., Langdon, S., Møkgolele, M.: A high frequency boundary element method for scattering by convex polygons with impedance boundary conditions. *Commun. Comput. Phys.* **11**, 573–593 (2012)
18. Chandler-Wilde, S.N., Langdon, S., Ritter, L.: A high-wavenumber boundary-element method for an acoustic scattering problem. *Philos. Trans. R. Soc. Lond. Ser. A* **362**(1816), 647–671 (2004)
19. Chandler-Wilde, S.N., Monk, P.: Wave-number-explicit bounds in time-harmonic scattering. *SIAM J. Math. Anal.* **39**(5), 1428–1455 (2008)
20. Colton, D., Kress, R.: Inverse Acoustic and Electromagnetic Scattering Theory. Springer-Verlag, Berlin (1992)
21. Colton, D.L., Kress, R.: Integral Equation Methods in Scattering Theory. John Wiley & Sons Inc., New York (1983)
22. Davis, C.P., Chew, W.C.: Frequency-independent scattering from a flat strip with TE_z -polarized fields. *IEEE Trans. Ant. Prop.* **56**, 1008–1016 (2008)
23. Domínguez, V., Graham, I.G., Smyshlyaev, V.P.: A hybrid numerical-asymptotic boundary integral method for high-frequency acoustic scattering. *Numer. Math.* **106**(3), 471–510 (2007)
24. Ecevit, F.: Integral equation formulations of electromagnetic and acoustic scattering problems: convergence of multiple scattering iterations and high-frequency asymptotic expansions. Ph.D. thesis, University of Minnesota (2005)
25. Ecevit, F., Reitich, F.: Analysis of multiple scattering iterations for high-frequency scattering problems. Part I: the two-dimensional case. *Numer. Math.* **114**, 271–354 (2009)
26. Ganesh, M., Hawkins, S.: A fully discrete Galerkin method for high frequency exterior acoustic scattering in three dimensions. *J. Comput. Phys.* **230**, 104–125 (2011)
27. Geuzaine, C., Bruno, O., Reitich, F.: On the $O(1)$ solution of multiple-scattering problems. *IEEE Trans. Magn.* **41**, 1488–1491 (2005)

28. Hewett, D.P., Langdon, S., Melenk, J.M.: A high frequency hp boundary element method for scattering by convex polygons. Submitted for publication - University of Reading preprint MPS-2011-18 (2011)
29. Keller, J.B.: Geometrical theory of diffraction. *J. Opt. Soc. Am. A* **52**, 116–130 (1962)
30. Kouyoumjian, R.G., Pathak, P.H.: A uniform geometrical theory of diffraction for an edge in a perfectly conducting surface. *P. IEEE* **62**(11), 1448–1461 (1974)
31. Kress, R.: Minimizing the condition number of boundary integral operators in acoustic and electromagnetic scattering. *Quart. J. Mech. Appl. Math.* **38**(2), 323 (1985)
32. Langdon, S., Chandler-Wilde, S.N.: A wavenumber independent boundary element method for an acoustic scattering problem. *SIAM J. Numer. Anal.* **43**(6), 2450–2477 (2006)
33. Langdon, S., Mokgolele, M., Chandler-Wilde, S.N.: High frequency scattering by convex curvilinear polygons. *J. Comput. Appl. Math.* **234**(6), 2020–2026 (2010)
34. Oberhettinger, F.: On asymptotic series for functions occurring in the theory of diffraction of waves by wedges. *J. Math. Phys.* **34**, 245–255 (1956)
35. Schwab, C.: p - and hp - Finite Element Methods. Clarendon Press, Oxford (1998)
36. Spence, E.A., Chandler-Wilde, S.N., Graham, I.G., Smyshlyaev, V.P.: A new frequency-uniform coercive boundary integral equation for acoustic scattering. *Comm. Pure Appl. Math.* **64**(10), 1384–1415 (2011)
37. Stenger, F.: Numerical Methods Based on Sinc and Analytic Functions. Springer-Verlag (1993)
38. Titchmarsh, E.C.: Theory of Functions, 2nd ed. OUP (1939)
39. Uncles, R.J.: Numerical solution of acoustic scattering problems at intermediate frequencies. *J. Acoust. Soc. Am.* **60**, 266 (1976)